hp-adaptation driven by polynomial-degree-robust a posteriori error estimates for elliptic problems

Vít Dolejší, Alexandre Ern, Martin Vohralík

hp-adaptation driven by polynomial-degree-robust a posteriori error estimates for elliptic problems*

Vít Dolejší[(1)], *Alexandre Ern*[(2)], *Martin Vohralík*[(3)]

[(1)] Charles University Prague, Faculty of Mathematics and Physics, Sokolovská 83, 186 75 Praha, Czech Republic, (dolejsi@karlin.mff.cuni.cz)

[(2)] Université Paris-Est, CERMICS (ENPC), 77455 Marne-la-Vallée, France (ern@cermics.enpc.fr).

[(3)] INRIA Paris-Rocquencourt, B.P. 105, 78153 Le Chesnay, France (martin.vohralik@inria.fr)

Abstract

We devise and study experimentally adaptive strategies driven by a posteriori error estimates to select automatically both the space mesh and the polynomial degree in a numerical approximation of the Laplace equation in two space dimensions. The adaptation is based on equilibrated flux estimates. These estimates are presented here for inhomogeneous Dirichlet and Neumann boundary conditions and for spatially-varying polynomial degree; they deliver a global error upper bound with constant one and, up to data oscillation, error lower bounds on element patches with a (computable) generic constant independent of the mesh size and of the polynomial degree. We numerically asses the estimates and the hp-adaptive strategy using the interior penalty discontinuous Galerkin method. Asymptotic exactness is observed for all the symmetric, nonsymmetric, and incomplete variants on non-nested unstructured grids for a smooth solution. Exponential convergence rates are reported for the incomplete version on several benchmarks with a singular solution.

Keywords: Laplace equation, a posteriori error estimate, p-robustness, hp-refinement, inhomogeneous boundary conditions, discontinuous Galerkin

1 Introduction

A posteriori error estimates for elliptic problems have been studied for several decades. These estimates deliver global upper bounds for the discretization error as a Hilbertian sum of local (cellwise) error indicators that are computable solely from the discrete

*This work was partly supported by the ERC-CZ project MORE "MOdelling REvisited + MOdel REduction" LL1202. The research of V. Dolejší was supported by the Grant No. 13-00522S of the Czech Science Foundation. This author acknowledges also the membership in the Nečas Center for Mathematical Modeling ncmm.karlin.mff.cuni.cz.

solution. At the same time, they represent local error lower bounds, up to data oscillation, see, e.g., the recent textbook [31]. They can be devised under various forms. Among these, equilibrated flux error estimates offer the salient advantage of delivering error upper bounds with constant one. Such estimates are typically evaluated by solving local mixed finite element problems on element patches around mesh vertices, see [22, 11, 3, 17] and the references therein. Another attractive property of equilibrated flux a posteriori error estimates that was uncovered recently in the conforming finite element setting, see [2], is polynomial-degree-robustness, that is, the generic constant in the local error lower bound turns out to be uniform in the polynomial degree (it can only depend on the shape-regularity of the underlying meshes). This result stems from nontrivial properties of mixed finite element spaces, namely from a right inverse of the divergence operator [8, Corollary 3.4] and from a right inverse of the normal trace [9, Theorem 7.1], whose stability properties are uniform in the polynomial degree; this type of result is not expected to hold in the more popular setting of residual-based a posteriori error estimates. The polynomial-degree-robustness of equilibrated flux error estimates was extended recently in [18] to a unified setting encompassing many nonconforming discretizations as Crouzeix–Raviart finite elements, mixed finite elements, and interior penalty discontinuous Galerkin. Therein, the idea is to introduce, in addition to the flux reconstruction, a conforming potential reconstruction which is also built by solving local problems in element patches around vertices.

The recent advances on equilibrated flux a posteriori error estimates have been presented in the setting of homogeneous Dirichlet boundary conditions and for uniform polynomial degree. The first contribution of this work is to extend these estimates to the practical setting of inhomogeneous Dirichlet and Neumann boundary conditions and to cover discretizations with variable polynomial degree. These extensions turn out to be nontrivial: possibly different polynomial degrees need to be assigned to each patch when reconstructing the flux and the potential, the local mixed finite element problems have to be suitably modified on patches touching the boundary, and the local partition of unity which combines contributions from all the vertices of a given mesh cell has to be revisited. Herein, we still achieve global error upper bounds with constant one and polynomial-degree-robust local error lower bounds.

The second contribution of this work is to devise an hp-adaptive strategy driven by the above polynomial-degree-robust equilibrated flux a posteriori error estimates. Several criteria for determining whether it is preferable to perform h- (mesh) or p- (polynomial degree) refinement have been proposed over the years, see, e.g., [19, 20, 16, 24] and the references therein. Typically, it is natural to increase the polynomial degree when the solution is estimated to be sufficiently smooth, and to decrease the mesh size when the solution is estimated to be rather rough. Therefore, a key ingredient is an estimate of the local smoothness of the exact solution. In the present setting, we exploit the polynomial-degree-robustness of the estimate to devise a smoothness indicator based on the comparison of the error indicator for the current discrete solution and its local projection onto the discretization space with polynomial degree minus one. Such an approach is well-suited to discretizations by the discontinuous Galerkin method. We assess the hp-adaptive strategy, which also allows for mesh coarsening and for local decrease of the polynomial degree, using the incomplete interior penalty discontinuous Galerkin method on three benchmark problems with a locally singular exact solution. Our numerical results show that exponential convergence rates with respect to degrees of freedom can be achieved with the present strategy, in agreement with general theoretical results [27, 28, 1, 10, 29].

The paper is organized as follows. In Section 2, we briefly describe the setting and

introduce basic notation. In Section 3, we devise and analyze equilibrated flux a posteriori error estimates for inhomogeneous Dirichlet and Neumann boundary conditions and varying polynomial degree. We devote Section 4 to the hp-adaptive strategy and to salient implementation aspects. Finally, we discuss our numerical results in Section 5.

2 Setting

Let $\Omega \subset \mathbb{R}^2$ be a polygonal domain (open, bounded, and connected set). We suppose that $\partial\Omega$ is divided into two simply connected parts $\Gamma_{\rm D}$ and $\Gamma_{\rm N}$ with disjoint interiors, and we assume that $|\Gamma_{\rm D}| > 0$. We consider the Laplace equation: find $u : \Omega \to \mathbb{R}$ such that

$$-\Delta u = f \qquad \text{in } \Omega, \tag{2.1a}$$

$$-\nabla u\cdot\mathbf{n}_\Omega = \sigma_{\rm N} \qquad \text{on } \Gamma_{\rm N}, \tag{2.1b}$$

$$u = u_{\rm D} \qquad \text{on } \Gamma_{\rm D}. \tag{2.1c}$$

All what follows can be easily extended to the case where a Neumann condition is enforced on the whole boundary, by adding a zero-mean value constraint to the solution and assuming the usual compatibility condition between f and $\sigma_{\rm N}$.

Let $H^1(\Omega)$ denote the Sobolev space of $L^2(\Omega)$ functions with weak gradients in $[L^2(\Omega)]^2$. Then, $H^1_*(\Omega)$ (resp., $H^1_{*,{\rm D}}(\Omega)$) is composed of all functions in $H^1(\Omega)$ with zero trace (resp., with trace equal to $u_{\rm D}$) on $\Gamma_{\rm D}$. The variational formulation of (2.1) reads: find $u \in H^1_{*,{\rm D}}(\Omega)$ such that

$$(\nabla u, \nabla v) = (f, v) - \langle \sigma_{\rm N}, v\rangle_{\Gamma_{\rm N}} \qquad \forall v \in H^1_*(\Omega). \tag{2.2}$$

Here $(\cdot,\cdot)$ stands for the L^2-inner product; we denote by $\|\cdot\|$ the associated norm. Similarly, $\langle\cdot,\cdot\rangle$ stands for the L^2-inner product on $\partial\Omega$. We add an index to $(\cdot,\cdot)$ and $\langle\cdot,\cdot\rangle$ when a (proper) subset of Ω is considered. We suppose that $f \in L^2(\Omega)$, $\sigma_{\rm N} \in L^2(\Gamma_{\rm N})$, and $u_{\rm D} \in H^1(\Gamma_{\rm D})$, where $H^1(\Gamma_{\rm D})$ is the one-dimensional Sobolev space on the manifold $\Gamma_{\rm D}$.

Numerical discretizations of (2.2) typically rely on a partition $\mathcal{T}_h$ of Ω. We consider here matching triangulations in the sense of Ciarlet [7]; below, we will need $\mathcal{T}_h$ to be shape-regular in the sense that there exists a constant $\kappa_{\mathcal{T}} > 0$ such that the ratio h_K/ϱ_K is uniformly bounded by $\kappa_{\mathcal{T}}$ for all triangulations $\mathcal{T}_h$, where h_K is the diameter of K and ϱ_K the diameter of the largest ball inscribed in K. The edges of the mesh $\mathcal{T}_h$ form the set $\mathcal{E}_h$, with $\mathcal{E}_h^{\rm ext}$ the edges lying on the boundary of Ω. We suppose that the interior of each boundary edge lies entirely either in $\Gamma_{\rm D}$ or $\Gamma_{\rm N}$ and denote the corresponding subsets of $\mathcal{E}_h^{\rm ext}$ by $\mathcal{E}_h^{\rm ext,D}$ and $\mathcal{E}_h^{\rm ext,N}$, respectively. Similarly, $\mathcal{V}_h$ stands for all mesh vertices and $\mathcal{V}_h^{\rm ext,D}$ ($\mathcal{V}_h^{\rm ext,N}$ respectively) for the mesh vertices which lie on some Dirichlet (Neumann) boundary edge. Note that $\mathcal{V}_h^{\rm ext,D} \cap \mathcal{V}_h^{\rm ext,N}$ is not empty unless $\Gamma_{\rm D} = \partial\Omega$; vertices on the interface between $\Gamma_{\rm D}$ and $\Gamma_{\rm N}$ lie both in $\mathcal{V}_h^{\rm ext,D}$ and $\mathcal{V}_h^{\rm ext,N}$ in our notation. We will consider the subset $\mathcal{V}_h^{\rm ext,D}$ for the flux reconstruction and the subset $\mathcal{V}_h^{\rm ext,N}$ for the potential reconstruction. We also denote by $\mathcal{V}_K$ the vertices of the element $K \in \mathcal{T}_h$ and by $\mathcal{V}_e$ the vertices of the edge $e \in \mathcal{E}_h$. Finally, all edges of an element $K \in \mathcal{T}_h$ are denoted by $\mathcal{E}_K$ and those edges that lie in $\Gamma_{\rm D}$ ($\Gamma_{\rm N}$) by $\mathcal{E}_K^{\rm D}$ ($\mathcal{E}_K^{\rm N}$). The jump operator $[\![\cdot]\!]$ yields the difference of the traces of the argument from the two mesh elements that share $e \in \mathcal{E}_h^{\rm int}$ (evaluated along a fixed unit normal $\mathbf{n}_e$ of e) and the actual trace on $e \in \mathcal{E}_h^{\rm ext}$. Similarly, the average operator $\{\!\{\cdot\}\!\}$ yields

the mean value of the traces from adjacent mesh elements on inner edges and the actual trace on boundary edges.

Let $\mathrm{R}_{\frac{\pi}{2}} := \begin{pmatrix} 0 & -1 \\ 1 & 0 \end{pmatrix}$ be the matrix of rotation by $\frac{\pi}{2}$. We use the convention $\mathrm{R}_{\frac{\pi}{2}}\mathbf{n}_\Omega = \mathbf{t}_\Omega$ to link the unit exterior normal and tangential vectors, and similarly on subdomains of Ω. We let

$$H^1(\mathcal{T}_h) := \{v \in L^2(\Omega);\, v|_K \in H^1(K)\ \forall K \in \mathcal{T}_h\}$$

be the broken Sobolev space and denote the broken (elementwise) weak gradient by ∇. Similarly, $\nabla\cdot$ stands for the broken weak divergence and $\mathrm{R}_{\frac{\pi}{2}}\nabla$ for the broken weak curl, $(\mathrm{R}_{\frac{\pi}{2}}\nabla v)|_K = (-\partial_y v, \partial_x v)^t|_K$ for $v \in H^1(\mathcal{T}_h)$ and all $K \in \mathcal{T}_h$. Let V be a finite-dimensional subspace of $L^2(\Omega)$; then we denote by Π_V the $L^2(\Omega)$-orthogonal projection onto V, and similarly on various subsets of Ω. We will also denote by Π_e^0 the $L^2(e)$-orthogonal projection onto constants.

3 Equilibrated flux a posteriori error estimates for inhomogeneous boundary conditions and varying polynomial degree

We present in this section a posteriori error estimates of equilibrated flux type, which extend previous results to inhomogeneous boundary conditions and varying polynomial degree.

3.1 Potential and flux reconstructions

Let $u_h \in H^1(\mathcal{T}_h)$ be the approximate solution. Let $\mathfrak{G}(u_h) \in [L^2(\Omega)]^2$ represent its gradient: typically, either $\mathfrak{G}(u_h)$ is given by the broken weak gradient ∇u_h or by a discrete gradient also taking into account the jumps in u_h, see (3.27) below for an example. In practice, u_h and $\mathfrak{G}(u_h)$ are piecewise polynomials, see assumption (3.30) below. They come from a specific numerical method, cf. Section 4.1. In general, $u_h \notin H^1(\Omega)$ and $-\mathfrak{G}(u_h) \notin \mathbf{H}(\mathrm{div}, \Omega)$, the space of $[L^2(\Omega)]^2$ functions with weak divergences in $L^2(\Omega)$, which leads us to:

Definition 3.1 (Potential reconstruction)**.** *We call a* potential reconstruction *any function s_h constructed from u_h which satisfies*

$$s_h \in H^1(\Omega) \cap C^0(\overline{\Omega}), \tag{3.1a}$$

$$s_h(\mathbf{a}) = u_{\mathrm{D}}(\mathbf{a}) \quad \forall \mathbf{a} \in \mathcal{V}_h^{\mathrm{ext,D}}. \tag{3.1b}$$

Definition 3.2 (Equilibrated flux reconstruction)**.** *We call an* equilibrated flux reconstruction *any function $\boldsymbol{\sigma}_h$ constructed from $\mathfrak{G}(u_h)$ which satisfies*

$$\boldsymbol{\sigma}_h \in \mathbf{H}(\mathrm{div}, \Omega), \tag{3.2a}$$

$$(\nabla\cdot\boldsymbol{\sigma}_h, 1)_K = (f, 1)_K \quad \forall K \in \mathcal{T}_h, \tag{3.2b}$$

$$\langle \boldsymbol{\sigma}_h\cdot\mathbf{n}_\Omega, 1\rangle_e = \langle \sigma_{\mathrm{N}}, 1\rangle_e \ \ \forall e \in \mathcal{E}_h^{\mathrm{ext,N}}. \tag{3.2c}$$

The continuity of s_h imposed in (3.1a) is needed in (3.1b) to take point values; we also notice that (3.2c) requires that $\boldsymbol{\sigma}_h\cdot\mathbf{n}_e|_e \in L^1(e)$ for all $e \in \mathcal{E}_h^{\mathrm{ext,N}}$. In practice, s_h and $\boldsymbol{\sigma}_h$ are piecewise polynomials, so that these requirements are readily met.

3.2 A general a posteriori error estimate

Our first important result is the generalization of [18, Theorem 3.3] to problem (2.1). Recall that if K is a triangle from the mesh $\mathcal{T}_h$ and e one of its edges, the following trace inequality holds:

$$\|v - \Pi_e^0 v\|_e \leq C_{\mathrm{t},K,e} h_e^{1/2} \|\nabla v\|_K \qquad \forall v \in H^1(K). \tag{3.3}$$

It is shown in [25, Lemma 3.5] that $C_{\mathrm{t},K,e}^2 = C_\mathrm{t} h_K^2/|K|$, where $C_\mathrm{t} \approx 0.77708$.

Theorem 3.3 (General a posteriori error estimate)**.** *Let u be the weak solution of (2.2). Let $u_h \in H^1(\mathcal{T}_h)$ be an arbitrary approximation of u, with $\mathfrak{G}(u_h) \in [L^2(\Omega)]^2$ an approximation of ∇u. Let s_h be a potential reconstruction in the sense of Definition 3.1 and $\boldsymbol{\sigma}_h$ an equilibrated flux reconstruction in the sense of Definition 3.2. Then,*

$$\|\nabla u - \mathfrak{G}(u_h)\|^2 \leq \eta^2 := \sum_{K\in\mathcal{T}_h} \eta_K^2 \tag{3.4a}$$

with

$$\eta_K^2 := \Bigg(\underbrace{\|\mathfrak{G}(u_h) + \boldsymbol{\sigma}_h\|_K}_{\eta_{\mathrm{CR},K},\,\text{constitutive rel.}} + \underbrace{\frac{h_K}{\pi}\|f - \nabla\cdot\boldsymbol{\sigma}_h\|_K}_{\eta_{\mathrm{osc},K},\,\text{data osc.}} + \underbrace{\sum_{e\in\mathcal{E}_K^\mathrm{N}} C_{\mathrm{t},K,e} h_e^{1/2} \|\boldsymbol{\sigma}_h\cdot\mathbf{n}_\Omega - \sigma_\mathrm{N}\|_e}_{\eta_{\Gamma_\mathrm{N},K},\,\text{Neumann BC}} \Bigg)^2$$
$$+ \Bigg(\underbrace{\|\mathfrak{G}(u_h) - \nabla s_h\|_K}_{\eta_{\mathrm{NC},K},\,\text{pot. nonconformity}} + \underbrace{\min_{\substack{v\in H^1(K),\\ v|_{\partial K\cap\Gamma_\mathrm{D}} = u_\mathrm{D} - s_h \\ v|_{\partial K\setminus\Gamma_\mathrm{D}} = 0}} \|\nabla v\|_K}_{\eta_{\Gamma_\mathrm{D},K},\,\text{Dirichlet BC}} \Bigg)^2. \tag{3.4b}$$

Proof. Let $s \in H^1_{*,\mathrm{D}}(\Omega)$ be such that $(\nabla s, \nabla v) = (\mathfrak{G}(u_h), \nabla v)$ for all $v \in H^1_*(\Omega)$. This leads to the Pythagorean equality

$$\|\nabla u - \mathfrak{G}(u_h)\|^2 = \|\nabla(u-s)\|^2 + \|\nabla s - \mathfrak{G}(u_h)\|^2. \tag{3.5}$$

The first term in (3.5) can be rewritten as follows, since $(u-s) \in H^1_*(\Omega)$:

$$\begin{aligned}
\|\nabla(u-s)\| &= \sup_{\varphi\in H^1_*(\Omega);\,\|\nabla\varphi\|=1} (\nabla(u-s), \nabla\varphi), \\
&= \sup_{\varphi\in H^1_*(\Omega);\,\|\nabla\varphi\|=1} (\nabla u - \mathfrak{G}(u_h), \nabla\varphi), \\
&= \sup_{\varphi\in H^1_*(\Omega);\,\|\nabla\varphi\|=1} \{(f,\varphi) - \langle\sigma_\mathrm{N},\varphi\rangle_{\Gamma_\mathrm{N}} - (\mathfrak{G}(u_h), \nabla\varphi)\},
\end{aligned}$$

where we have used the definition of s and (2.2). Fix $\varphi \in H^1_*(\Omega)$ with $\|\nabla\varphi\| = 1$. Adding and subtracting $(\boldsymbol{\sigma}_h, \nabla\varphi)$, where $\boldsymbol{\sigma}_h$ is the equilibrated flux reconstruction in the sense of Definition 3.2, and using the Green theorem, we infer that

$$(f,\varphi) - \langle\sigma_\mathrm{N},\varphi\rangle_{\Gamma_\mathrm{N}} - (\mathfrak{G}(u_h),\nabla\varphi) = (f - \nabla\cdot\boldsymbol{\sigma}_h, \varphi) + \langle\boldsymbol{\sigma}_h\cdot\mathbf{n}_\Omega - \sigma_\mathrm{N}, \varphi\rangle_{\Gamma_\mathrm{N}} - (\mathfrak{G}(u_h) + \boldsymbol{\sigma}_h, \nabla\varphi).$$

The first and last terms above are treated exactly as in the proof of [18, Theorem 3.3],

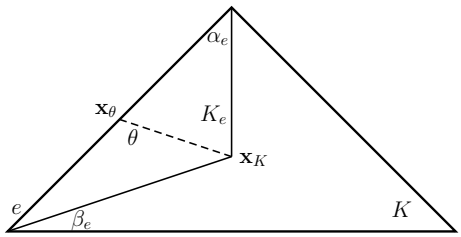

Fig. 1: Notation for the inhomogeneous Dirichlet boundary condition estimate

using in particular the equilibration (3.2b). For the middle term, we observe that

$$\begin{aligned}\langle \boldsymbol{\sigma}_h\cdot\mathbf{n}_\Omega - \sigma_{\mathrm{N}}, \varphi\rangle_{\Gamma_{\mathrm{N}}} &= \sum_{K\in\mathcal{T}_h}\sum_{e\in\mathcal{E}_K^{\mathrm{N}}} \langle \boldsymbol{\sigma}_h\cdot\mathbf{n}_\Omega - \sigma_{\mathrm{N}}, \varphi\rangle_e \\ &= \sum_{K\in\mathcal{T}_h}\sum_{e\in\mathcal{E}_K^{\mathrm{N}}} \langle \boldsymbol{\sigma}_h\cdot\mathbf{n}_\Omega - \sigma_{\mathrm{N}}, \varphi - \Pi_e^0\varphi\rangle_e \\ &\le \sum_{K\in\mathcal{T}_h}\sum_{e\in\mathcal{E}_K^{\mathrm{N}}} \left\{\|\boldsymbol{\sigma}_h\cdot\mathbf{n}_\Omega - \sigma_{\mathrm{N}}\|_e C_{\mathrm{t},K,e} h_e^{1/2}\|\nabla\varphi\|_K\right\},\end{aligned}$$

owing to (3.2c), the Cauchy–Schwarz inequality, and (3.3). Note that only those elements having (at least) one face located on the Neumann boundary are concerned. This leads to the terms composing the first line of (3.4b).

Consider now the second term in (3.5). Proceeding as in [21, Section 4.1], we infer that

$$\begin{aligned}\|\nabla s - \mathfrak{G}(u_h)\|^2 &= \min_{w\in H^1_{*,\mathrm{D}}(\Omega)} \|\nabla w - \mathfrak{G}(u_h)\|^2 \\ &\le \min_{w\in H^1_{*,\mathrm{D}}(\Omega)} \sum_{K\in\mathcal{T}_h} \left(\|\nabla s_h - \mathfrak{G}(u_h)\|_K + \|\nabla(w-s_h)\|_K\right)^2 \\ &\le \sum_{K\in\mathcal{T}_h} \left(\|\nabla s_h - \mathfrak{G}(u_h)\|_K + \min_{\substack{w\in H^1(K),\\ w|_{\partial K\cap\Gamma_{\mathrm{D}}}=u_{\mathrm{D}}\\ w|_{\partial K\setminus\Gamma_{\mathrm{D}}}=s_h}} \|\nabla(w-s_h)\|_K\right)^2,\end{aligned}$$

where the first inequality follows by localization on mesh elements and the triangle inequality, and the second one by restricting the global minimum to elementwise minima over functions $w\in H^1(K)$ with values on ∂K fixed respectively to u_{D} or s_h, thanks to conditions (3.1a) and (3.1b). Note that the elements concerned by the minimization are those having (at least) one edge located on the Dirichlet boundary. This leads to the terms composing the second line of (3.4b). □

The expression for the general Dirichlet boundary condition error from Theorem 3.3 is not computable. We now derive a computable upper bound for this quantity. The proof is skipped since it follows that in [6, Theorem 5.1]; it consists in bounding the minimum by considering a function given by the Dirichlet boundary misfit on the concerned edges and extending it linearly to zero at the cell barycenter using polar coordinates.

Theorem 3.4 (Inhomogeneous Dirichlet boundary condition estimate)**.** *Let $K \in \mathcal{T}_h$ be such that $|\partial K \cap \Gamma_{\mathrm{D}}| > 0$. Let $\mathbf{x}_K$ denote the barycenter of K. For each $e \in \mathcal{E}_K^{\mathrm{D}}$, consider the polar coordinates r, θ centered at $\mathbf{x}_K$, where the triangle K_e given by the edge e and the point $\mathbf{x}_K$ is described by $\theta \in [\alpha_e, \beta_e]$ and $r \in [0, R_e(\theta)]$; $R_e(\theta)$ is thus the distance of $\mathbf{x}_K$ and $\mathbf{x}_\theta \in e$, see Figure 1. Set $g_e(\theta) := (u_{\mathrm{D}} - s_h)(\mathbf{x}_\theta)$ and denote by $'$ the differentiation with respect to θ. Then*

$$\min_{\substack{v \in H^1(K),\\ v|_{\partial K \cap \Gamma_{\mathrm{D}}} = u_{\mathrm{D}} - s_h \\ v|_{\partial K \setminus \Gamma_{\mathrm{D}}} = 0}} \|\nabla v\|_K \leq \sum_{e \in \mathcal{E}_K^{\mathrm{D}}} \left\{ \frac{1}{2} \int_{\alpha_e}^{\beta_e} \left\{ [g_e(\theta)]^2 + [(g_e'(\theta) R_e(\theta) - g_e(\theta) R_e'(\theta))/R_e(\theta)]^2 \right\} \mathrm{d}\theta \right\}^{1/2}.$$

This computable estimate is of higher order whenever u_{D} has enough regularity, see the discussions in [21, 6].

3.3 Reconstructions from local problems with variable polynomial degree

In this section, we extend the material of [18, Section 3.1.3] to potential and flux reconstructions where each element patch around a mesh vertex can be assigned a specific polynomial degree. For a vertex $\mathbf{a} \in \mathcal{V}_h$, let $\mathcal{T}_{\mathbf{a}}$ denote the patch of elements of $\mathcal{T}_h$ which share $\mathbf{a}$, and let $\omega_{\mathbf{a}}$ be the corresponding open subdomain of diameter $h_{\omega_{\mathbf{a}}}$. We denote by $\psi_{\mathbf{a}}$ the continuous piecewise affine "hat" function, taking the value 1 at the vertex $\mathbf{a}$ and 0 at the other vertices. We assign a polynomial degree $p_{\mathbf{a}} \geq 0$ to each vertex $\mathbf{a} \in \mathcal{V}_h$. Then, we let $\mathbf{V}_h(\omega_{\mathbf{a}})$ be the Raviart–Thomas mixed finite element space of degree $p_{\mathbf{a}}$ on the mesh $\mathcal{T}_{\mathbf{a}}$ of $\omega_{\mathbf{a}}$; functions in this space belong elementwise to $[\mathbb{P}_{p_{\mathbf{a}}}(K)]^2 + \mathbb{P}_{p_{\mathbf{a}}}(K)\mathbf{x}$ and their normal trace over the edges inside $\mathcal{T}_{\mathbf{a}}$ is in $\mathbb{P}_{p_{\mathbf{a}}}(e)$ and is continuous [5, 26]. Let $Q_h(\omega_{\mathbf{a}})$ be the space of discontinuous piecewise polynomials on $\mathcal{T}_{\mathbf{a}}$ of degree $p_{\mathbf{a}}$. We remark that Brezzi–Douglas–Marini spaces can also be considered, see [18, Remark 3.21].

The reconstruction of an equilibrated flux $\boldsymbol{\sigma}_h$ following Definition 3.2, for varying polynomial degree and general boundary conditions, takes the following form:

Definition 3.5 (Flux reconstruction $\boldsymbol{\sigma}_h$)**.** *Assume that $\mathfrak{G}(u_h)$ satisfies the hat-function orthogonality*

$$(\mathfrak{G}(u_h), \nabla\psi_{\mathbf{a}})_{\omega_{\mathbf{a}}} = (f, \psi_{\mathbf{a}})_{\omega_{\mathbf{a}}} - \langle \sigma_{\mathrm{N}}, \psi_{\mathbf{a}} \rangle_{\Gamma_{\mathrm{N}}} \qquad \forall \mathbf{a} \in \mathcal{V}_h \setminus \mathcal{V}_h^{\mathrm{ext,D}}. \tag{3.6}$$

For each $\mathbf{a} \in \mathcal{V}_h$, prescribe $\boldsymbol{\varsigma}_h^{\mathbf{a}} \in \mathbf{V}_{h,\mathrm{N}}^{\mathbf{a}}$ and $\bar{r}_h^{\mathbf{a}} \in Q_h^{\mathbf{a}}$ by solving

$$(\boldsymbol{\varsigma}_h^{\mathbf{a}}, \mathbf{v}_h)_{\omega_{\mathbf{a}}} - (\bar{r}_h^{\mathbf{a}}, \nabla\cdot\mathbf{v}_h)_{\omega_{\mathbf{a}}} = -(\psi_{\mathbf{a}}\mathfrak{G}(u_h), \mathbf{v}_h)_{\omega_{\mathbf{a}}} \qquad \forall \mathbf{v}_h \in \mathbf{V}_h^{\mathbf{a}}, \tag{3.7a}$$

$$(\nabla\cdot\boldsymbol{\varsigma}_h^{\mathbf{a}}, q_h)_{\omega_{\mathbf{a}}} = (\psi_{\mathbf{a}} f - \nabla\psi_{\mathbf{a}}\cdot\mathfrak{G}(u_h), q_h)_{\omega_{\mathbf{a}}} \qquad \forall q_h \in Q_h^{\mathbf{a}} \tag{3.7b}$$

with the following spaces: for all $\mathbf{a} \in \mathcal{V}_h^{\mathrm{int}}$,

$$\mathbf{V}_{h,\mathrm{N}}^{\mathbf{a}} := \mathbf{V}_h^{\mathbf{a}} := \{\mathbf{v}_h \in \mathbf{V}_h(\omega_{\mathbf{a}});\ \mathbf{v}_h\cdot\mathbf{n}_{\omega_{\mathbf{a}}}|_{\partial\omega_{\mathbf{a}}} = 0\}, \tag{3.8a}$$

$$Q_h^{\mathbf{a}} := \{q_h \in Q_h(\omega_{\mathbf{a}});\ (q_h, 1)_{\omega_{\mathbf{a}}} = 0\}, \tag{3.8b}$$

and, for all $\mathbf{a} \in \mathcal{V}_h^{\rm ext}$*, with* $\tilde{g}_{\rm N}^{\mathbf{a}} := \Pi_{\mathbf{V}_h(\omega_{\mathbf{a}})\cdot\mathbf{n}}(\psi_{\mathbf{a}}\sigma_{\rm N})$*,*

$$\mathbf{V}_{h,{\rm N}}^{\mathbf{a}} := \{\mathbf{v}_h \in \mathbf{V}_h(\omega_{\mathbf{a}});\ \mathbf{v}_h\cdot\mathbf{n}_{\omega_{\mathbf{a}}}|_{\partial\omega_{\mathbf{a}}\setminus\partial\Omega} = 0,\ \mathbf{v}_h\cdot\mathbf{n}_{\omega_{\mathbf{a}}}|_{\partial\omega_{\mathbf{a}}\cap\Gamma_{\rm N}} = \tilde{g}_{\rm N}^{\mathbf{a}}\}, \tag{3.9a}$$

$$\mathbf{V}_h^{\mathbf{a}} := \{\mathbf{v}_h \in \mathbf{V}_h(\omega_{\mathbf{a}});\ \mathbf{v}_h\cdot\mathbf{n}_{\omega_{\mathbf{a}}}|_{\partial\omega_{\mathbf{a}}\setminus\partial\Omega} = 0,\ \mathbf{v}_h\cdot\mathbf{n}_{\omega_{\mathbf{a}}}|_{\partial\omega_{\mathbf{a}}\cap\Gamma_{\rm N}} = 0\}, \tag{3.9b}$$

while

$$Q_h^{\mathbf{a}} := \{q_h \in Q_h(\omega_{\mathbf{a}});\ (q_h,1)_{\omega_{\mathbf{a}}} = 0\} \quad \mathbf{a} \in \mathcal{V}_h^{\rm ext}\setminus\mathcal{V}_h^{\rm ext,D}, \tag{3.10a}$$

$$Q_h^{\mathbf{a}} := Q_h(\omega_{\mathbf{a}}) \qquad\qquad\qquad\quad \mathbf{a} \in \mathcal{V}_h^{\rm ext,D}. \tag{3.10b}$$

Then, set

$$\boldsymbol{\sigma}_h := \sum_{\mathbf{a}\in\mathcal{V}_h} \boldsymbol{\varsigma}_h^{\mathbf{a}}. \tag{3.11}$$

The above local problems only differ from those of [18, Construction 3.4] for vertices which lie on the Neumann boundary $\Gamma_{\rm N}$, i.e., whenever $\mathbf{a}$ lies on $\partial\Omega$ and $|\partial\omega_{\mathbf{a}}\cap\Gamma_{\rm N}| > 0$. In the present setting, an inhomogeneous Neumann boundary condition is encoded in the space $\mathbf{V}_{h,{\rm N}}^{\mathbf{a}}$ of (3.9a) whereby $\boldsymbol{\varsigma}_h^{\mathbf{a}}\cdot\mathbf{n}_{\omega_{\mathbf{a}}}|_{\partial\omega_{\mathbf{a}}\cap\Gamma_{\rm N}}$ is enforced to be the polynomial projection of $\psi_{\mathbf{a}}\sigma_{\rm N}$ onto the space of normal traces of the local mixed finite element space $\mathbf{V}_h(\omega_{\mathbf{a}})$. Problem (3.7) for $\mathbf{a} \in \mathcal{V}_h^{\rm ext}$ is a pure Neumann problem when $\partial\omega_{\mathbf{a}}\cap\Gamma_{\rm N} = \partial\omega_{\mathbf{a}}\cap\partial\Omega$, i.e., when the whole boundary of $\omega_{\mathbf{a}}$ lying on $\partial\Omega$ is on the Neumann boundary. This happens if and only if $\mathbf{a} \in \mathcal{V}_h^{\rm ext}\setminus\mathcal{V}_h^{\rm ext,D}$. The Neumann compatibility condition then requests that

$$(\psi_{\mathbf{a}} f - \nabla\psi_{\mathbf{a}}\cdot\mathfrak{G}(u_h),1)_{\omega_{\mathbf{a}}} = \langle\Pi_{\mathbf{V}_h(\omega_{\mathbf{a}})\cdot\mathbf{n}}(\psi_{\mathbf{a}}\sigma_{\rm N}),1\rangle_{\partial\omega_{\mathbf{a}}\cap\Gamma_{\rm N}}. \tag{3.12}$$

Noting that $\langle\Pi_{\mathbf{V}_h(\omega_{\mathbf{a}})\cdot\mathbf{n}}(\psi_{\mathbf{a}}\sigma_{\rm N}),1\rangle_{\partial\omega_{\mathbf{a}}\cap\Gamma_{\rm N}} = \langle\psi_{\mathbf{a}}\sigma_{\rm N},1\rangle_{\Gamma_{\rm N}}$, this is nothing but (3.6) for $\mathbf{a} \in \mathcal{V}_h^{\rm ext}\setminus\mathcal{V}_h^{\rm ext,D}$. Shall $|\partial\omega_{\mathbf{a}}\cap\Gamma_{\rm D}| > 0$ for a boundary vertex, we have a local Neumann–Dirichlet problem, with the normal trace of $\boldsymbol{\varsigma}_h^{\mathbf{a}}$ not prescribed on $\partial\omega_{\mathbf{a}}\cap\Gamma_{\rm D}$.

Lemma 3.6 (Properties of $\boldsymbol{\sigma}_h$)**.** *The following holds:*

$$\boldsymbol{\sigma}_h \in \mathbf{H}(\mathrm{div},\Omega), \tag{3.13a}$$

$$(f - \nabla\cdot\boldsymbol{\sigma}_h, v_h)_K = 0 \qquad \forall K \in \mathcal{T}_h,\ \forall v_h \in \mathbb{P}_{\min_{\mathbf{a}\in\mathcal{V}_K} p_{\mathbf{a}}}(K), \tag{3.13b}$$

$$\langle\boldsymbol{\sigma}_h\cdot\mathbf{n}_\Omega - \sigma_{\rm N}, v_h\rangle_e = 0 \quad \forall e \in \mathcal{E}_h^{\rm ext,N},\ \forall v_h \in \mathbb{P}_{\min_{\mathbf{a}\in\mathcal{V}_e} p_{\mathbf{a}}}(e). \tag{3.13c}$$

Thus, in particular the three properties in (3.2) *are satisfied.*

Proof. The first two properties are proved as in [18, Lemma 3.5]. Let $e \in \mathcal{E}_h^{\rm ext,N}$ and let $v_h \in \mathbb{P}_{\min_{\mathbf{a}\in\mathcal{V}_e} p_{\mathbf{a}}}(e)$. Employing that $\boldsymbol{\sigma}_h|_e = \sum_{\mathbf{a}\in\mathcal{V}_e}\boldsymbol{\varsigma}_h^{\mathbf{a}}$ and using the normal trace condition imposed on $\mathbf{V}_{h,{\rm N}}^{\mathbf{a}}$ in (3.9a), we infer that $\langle\boldsymbol{\sigma}_h\cdot\mathbf{n}_\Omega, v_h\rangle_e = \sum_{\mathbf{a}\in\mathcal{V}_e}\langle\boldsymbol{\varsigma}_h^{\mathbf{a}}\cdot\mathbf{n}_\Omega, v_h\rangle_e = \sum_{\mathbf{a}\in\mathcal{V}_e}\langle\psi_{\mathbf{a}}\sigma_{\rm N}, v_h\rangle_e = \langle\sigma_{\rm N}, v_h\rangle_e$. □

Remark 3.7 (Local flux minimization)**.** *Similarly to [18, Remark 3.7], Definition 3.5 can be equivalently stated as:*

$$\boldsymbol{\varsigma}_h^{\mathbf{a}} := \arg\min_{\mathbf{v}_h\in\mathbf{V}_{h,{\rm N}}^{\mathbf{a}},\ \nabla\cdot\mathbf{v}_h = \Pi_{Q_h^{\mathbf{a}}}(\psi_{\mathbf{a}} f - \nabla\psi_{\mathbf{a}}\cdot\mathfrak{G}(u_h))} \|\psi_{\mathbf{a}}\mathfrak{G}(u_h) + \mathbf{v}_h\|_{\omega_{\mathbf{a}}} \qquad \forall\mathbf{a} \in \mathcal{V}_h. \tag{3.14}$$

We now turn to the potential reconstruction. We can construct s_h via the same local problems (3.7), upon merely replacing the right-hand sides and adjusting the spaces $\mathbf{V}_h^{\mathbf{a}}$ and $Q_h^{\mathbf{a}}$ close to the boundary. This turns out to be equivalent to a primal conforming finite element solve, see Remark 3.10 below.

Definition 3.8 (Potential reconstruction s_h)**.** *For each* $\mathbf{a} \in \mathcal{V}_h$*, prescribe* $\boldsymbol{\varsigma}_h^{\mathbf{a}} \in \mathbf{V}_{h,\mathrm{N}}^{\mathbf{a}}$ *and* $\bar{r}_h^{\mathbf{a}} \in Q_h^{\mathbf{a}}$ *by solving*

$$(\boldsymbol{\varsigma}_h^{\mathbf{a}}, \mathbf{v}_h)_{\omega_{\mathbf{a}}} - (\bar{r}_h^{\mathbf{a}}, \nabla\cdot\mathbf{v}_h)_{\omega_{\mathbf{a}}} = -(\mathrm{R}_{\frac{\pi}{2}}\nabla(\psi_{\mathbf{a}}u_h), \mathbf{v}_h)_{\omega_{\mathbf{a}}} \qquad \forall \mathbf{v}_h \in \mathbf{V}_h^{\mathbf{a}}, \tag{3.15a}$$

$$(\nabla\cdot\boldsymbol{\varsigma}_h^{\mathbf{a}}, q_h)_{\omega_{\mathbf{a}}} = 0 \qquad \forall q_h \in Q_h^{\mathbf{a}} \tag{3.15b}$$

with the following spaces: for all $\mathbf{a} \in \mathcal{V}_h^{\mathrm{int}}$*,*

$$\mathbf{V}_{h,\mathrm{N}}^{\mathbf{a}} := \mathbf{V}_h^{\mathbf{a}} := \{\mathbf{v}_h \in \mathbf{V}_h(\omega_{\mathbf{a}});\ \mathbf{v}_h\cdot\mathbf{n}_{\omega_{\mathbf{a}}}|_{\partial\omega_{\mathbf{a}}} = 0\}, \tag{3.16a}$$

$$Q_h^{\mathbf{a}} := \{q_h \in Q_h(\omega_{\mathbf{a}});\ (q_h, 1)_{\omega_{\mathbf{a}}} = 0\}, \tag{3.16b}$$

and, for all $\mathbf{a} \in \mathcal{V}_h^{\mathrm{ext}}$*, with* $\tilde{g}_{\mathrm{D}}^{\mathbf{a}} := \Pi_{\mathbf{V}_h(\omega_{\mathbf{a}})\cdot\mathbf{n}}(\nabla(\psi_{\mathbf{a}}u_{\mathrm{D}})\cdot\mathbf{t}_\Omega)$*,*

$$\mathbf{V}_{h,\mathrm{N}}^{\mathbf{a}} := \{\mathbf{v}_h \in \mathbf{V}_h(\omega_{\mathbf{a}});\ \mathbf{v}_h\cdot\mathbf{n}_{\omega_{\mathbf{a}}}|_{\partial\omega_{\mathbf{a}}\setminus\partial\Omega} = 0,\ \mathbf{v}_h\cdot\mathbf{n}_{\omega_{\mathbf{a}}}|_{\partial\omega_{\mathbf{a}}\cap\Gamma_{\mathrm{D}}} = \tilde{g}_{\mathrm{D}}^{\mathbf{a}}\}, \tag{3.17a}$$

$$\mathbf{V}_h^{\mathbf{a}} := \{\mathbf{v}_h \in \mathbf{V}_h(\omega_{\mathbf{a}});\ \mathbf{v}_h\cdot\mathbf{n}_{\omega_{\mathbf{a}}}|_{\partial\omega_{\mathbf{a}}\setminus\partial\Omega} = 0,\ \mathbf{v}_h\cdot\mathbf{n}_{\omega_{\mathbf{a}}}|_{\partial\omega_{\mathbf{a}}\cap\Gamma_{\mathrm{D}}} = 0\}, \tag{3.17b}$$

while

$$Q_h^{\mathbf{a}} := \{q_h \in Q_h(\omega_{\mathbf{a}});\ (q_h, 1)_{\omega_{\mathbf{a}}} = 0\} \quad \mathbf{a} \in \mathcal{V}_h^{\mathrm{ext}} \setminus \mathcal{V}_h^{\mathrm{ext,N}}, \tag{3.18a}$$

$$Q_h^{\mathbf{a}} := Q_h(\omega_{\mathbf{a}}) \qquad \mathbf{a} \in \mathcal{V}_h^{\mathrm{ext,N}}. \tag{3.18b}$$

Then, set

$$-\mathrm{R}_{\frac{\pi}{2}}\nabla s_h^{\mathbf{a}} := \boldsymbol{\varsigma}_h^{\mathbf{a}}, \tag{3.19a}$$

$$s_h^{\mathbf{a}}|_{\partial\omega_{\mathbf{a}}\setminus\partial\Omega} := 0, \tag{3.19b}$$

$$s_h := \sum_{\mathbf{a}\in\mathcal{V}_h} s_h^{\mathbf{a}}. \tag{3.19c}$$

Note that for boundary vertices $\mathbf{a} \in \mathcal{V}_h^{\mathrm{ext}} \setminus \mathcal{V}_h^{\mathrm{ext,N}}$ (which are such that $\partial\omega_{\mathbf{a}} \cap \Gamma_{\mathrm{D}} = \partial\omega_{\mathbf{a}} \cap \partial\Omega$, i.e., the whole boundary of $\omega_{\mathbf{a}}$ lying on $\partial\Omega$ is on the Dirichlet boundary), (3.15) is a pure Neumann problem: the normal trace of $\boldsymbol{\varsigma}_h^{\mathbf{a}}$ on $\partial\omega_{\mathbf{a}} \cap \Gamma_{\mathrm{D}}$ is prescribed by the (polynomial projection of the) tangential trace of $\nabla(\psi_{\mathbf{a}}u_{\mathrm{D}})$. The Neumann compatibility condition then requests that

$$\langle\tilde{g}_{\mathrm{D}}^{\mathbf{a}}, 1\rangle_{\partial\omega_{\mathbf{a}}\cap\Gamma_{\mathrm{D}}} = \langle\Pi_{\mathbf{V}_h(\omega_{\mathbf{a}})\cdot\mathbf{n}}(\nabla(\psi_{\mathbf{a}}u_{\mathrm{D}})\cdot\mathbf{t}_\Omega), 1\rangle_{\partial\omega_{\mathbf{a}}\cap\Gamma_{\mathrm{D}}} = 0. \tag{3.20}$$

This is immediate developing the above right-hand side since

$$\begin{aligned}\langle\tilde{g}_{\mathrm{D}}^{\mathbf{a}}, 1\rangle_{\partial\omega_{\mathbf{a}}\cap\Gamma_{\mathrm{D}}} &= -\langle\mathrm{R}_{\frac{\pi}{2}}\nabla(\psi_{\mathbf{a}}u_{\mathrm{D}})\cdot\mathbf{n}_\Omega, 1\rangle_{\partial\omega_{\mathbf{a}}\cap\Gamma_{\mathrm{D}}} = -\langle\mathrm{R}_{\frac{\pi}{2}}\nabla(\psi_{\mathbf{a}}u_{\mathrm{D}})\cdot\mathbf{n}_{\omega_{\mathbf{a}}}, 1\rangle_{\partial\omega_{\mathbf{a}}}\\ &= -(\nabla\cdot(\mathrm{R}_{\frac{\pi}{2}}\nabla(\psi_{\mathbf{a}}u_{\mathrm{D}})), 1)_{\omega_{\mathbf{a}}} - (\mathrm{R}_{\frac{\pi}{2}}\nabla(\psi_{\mathbf{a}}u_{\mathrm{D}}), \nabla 1)_{\omega_{\mathbf{a}}} = 0,\end{aligned} \tag{3.21}$$

for any smooth enough extension u_{D} of the Dirichlet boundary condition u_{D}. Shall $|\partial\omega_{\mathbf{a}} \cap \Gamma_{\mathrm{N}}| > 0$, (3.15) is a local Neumann–Dirichlet problem, with the normal trace of $\boldsymbol{\varsigma}_h^{\mathbf{a}}$ not prescribed on $\partial\omega_{\mathbf{a}} \cap \Gamma_{\mathrm{N}}$.

Lemma 3.9 (Properties of s_h)**.** *Conditions* (3.1a) *and* (3.1b) *are satisfied. Moreover, the following holds for all* $e \in \mathcal{E}_h^{\mathrm{ext,D}}$*:*

$$(\nabla s_h\cdot\mathbf{t}_\Omega)|_{\Gamma_{\mathrm{D}}} = \Pi_{\mathbb{P}_{\min_{\mathbf{a}\in\mathcal{V}_e} p_{\mathbf{a}}}(e)}(\nabla u_{\mathrm{D}}\cdot\mathbf{t}_\Omega)|_{\Gamma_{\mathrm{D}}}, \tag{3.22}$$

Proof. Condition (3.1a) is met by construction. We next show (3.22). Let $e \in \mathcal{E}_h^{\mathrm{ext,D}}$ and let $v_h \in \mathbb{P}_{\min_{\mathbf{a}\in\mathcal{V}_e} p_{\mathbf{a}}}(e)$. Since $-\mathrm{R}_{\frac{\pi}{2}}\nabla s_h = \sum_{\mathbf{a}\in\mathcal{V}_h} \boldsymbol{\varsigma}_h^{\mathbf{a}}$, using the normal trace condition imposed on $\mathbf{V}_{h,\mathrm{N}}^{\mathbf{a}}$ in (3.17a), we infer that

$$\langle -\mathrm{R}_{\frac{\pi}{2}}\nabla s_h\cdot\mathbf{n}_\Omega, v_h\rangle_e = \sum_{\mathbf{a}\in\mathcal{V}_e}\langle \boldsymbol{\varsigma}_h^{\mathbf{a}}\cdot\mathbf{n}_\Omega, v_h\rangle_e = \sum_{\mathbf{a}\in\mathcal{V}_e}\langle \nabla(\psi_{\mathbf{a}}u_{\mathrm{D}})\cdot\mathbf{t}_\Omega, v_h\rangle_e = \langle \nabla u_{\mathrm{D}}\cdot\mathbf{t}_\Omega, v_h\rangle_e,$$

and (3.22) follows from $-\mathrm{R}_{\frac{\pi}{2}}\nabla s_h\cdot\mathbf{n}_\Omega = \nabla s_h\cdot\mathbf{t}_\Omega$. To show (3.1b), we reason as follows: for each $\mathbf{a}\in\mathcal{V}_h^{\mathrm{ext,D}}$, $\nabla s_h^{\mathbf{a}}\cdot\mathbf{t}_\Omega$ preserves edgewise mean values of $\nabla(\psi_{\mathbf{a}}u_{\mathrm{D}})\cdot\mathbf{t}_\Omega$ for all $e\in\mathcal{E}_h^{\mathrm{ext,D}}$ contained in $\partial\omega_{\mathbf{a}}$. This follows as above by (3.19a) and (3.17a). Moreover, by (3.19b), $s_h^{\mathbf{a}}(\mathbf{a}') = 0 = (\psi_{\mathbf{a}}u_{\mathrm{D}})(\mathbf{a}')$ for the other vertices $\mathbf{a}'$ of $\omega_{\mathbf{a}}$ lying on $\partial\omega_{\mathbf{a}}\cap\Gamma_{\mathrm{D}}$. Thus, $s_h^{\mathbf{a}}(\mathbf{a}) = (\psi_{\mathbf{a}}u_{\mathrm{D}})(\mathbf{a}) = u_{\mathrm{D}}(\mathbf{a})$, and the conclusion follows by (3.19c). □

Remark 3.10 (Local potential minimization)**.** *Similarly to [18, Remark 3.10], Definition 3.8 can be equivalently stated as:*

$$\boldsymbol{\varsigma}_h^{\mathbf{a}} := \arg\min_{\mathbf{v}_h\in\mathbf{V}_{h,\mathrm{N}}^{\mathbf{a}},\,\nabla\cdot\mathbf{v}_h=0} \big\|\mathrm{R}_{\frac{\pi}{2}}\nabla(\psi_{\mathbf{a}}u_h) + \mathbf{v}_h\big\|_{\omega_{\mathbf{a}}} \qquad \forall\mathbf{a}\in\mathcal{V}_h. \tag{3.23}$$

Moreover, a discrete primal formulation is

$$s_h^{\mathbf{a}} := \arg\min_{v_h\in V_{h,\mathrm{D}}^{\mathbf{a}}} \|\nabla(\psi_{\mathbf{a}}u_h - v_h)\|_{\omega_{\mathbf{a}}} \qquad \forall\mathbf{a}\in\mathcal{V}_h, \tag{3.24}$$

where $V_{h,\mathrm{D}}^{\mathbf{a}}$ denotes piecewise polynomials on $\mathcal{T}_{\mathbf{a}}$ such that $\mathrm{R}_{\frac{\pi}{2}}\nabla V_{h,\mathrm{D}}^{\mathbf{a}} = \mathbf{V}_{h,\mathrm{N}}^{\mathbf{a}}$; in particular, there is a zero Dirichlet boundary condition on the whole $\partial\omega_{\mathbf{a}}$ for $\mathbf{a}\in\mathcal{V}_h^{\mathrm{int}}$, a zero Dirichlet boundary condition on $\partial\omega_{\mathbf{a}}\setminus\partial\Omega$ for $\mathbf{a}\in\mathcal{V}_h^{\mathrm{ext}}\setminus\mathcal{V}_h^{\mathrm{ext,D}}$, and, for $\mathbf{a}\in\mathcal{V}_h^{\mathrm{ext,D}}$, the Dirichlet boundary condition on $\partial\omega_{\mathbf{a}}\setminus\Gamma_{\mathrm{N}}$ is given by

$$\begin{aligned}(\nabla v_h\cdot\mathbf{t}_\Omega)|_e &= \Pi_{\mathbf{V}_h(\omega_{\mathbf{a}})\cdot\mathbf{n}_{\omega_{\mathbf{a}}}}(\nabla(\psi_{\mathbf{a}}u_{\mathrm{D}})\cdot\mathbf{t}_\Omega)|_e \qquad \forall e\in\mathcal{E}_h^{\mathrm{ext,D}},\ e\subset\partial\omega_{\mathbf{a}},\\ v_h(\mathbf{a}) &= u_{\mathrm{D}}(\mathbf{a}),\\ v_h|_{\partial\omega_{\mathbf{a}}\setminus\partial\Omega} &= 0.\end{aligned}$$

Let $V_h^{\mathbf{a}}$ be as $V_{h,\mathrm{D}}^{\mathbf{a}}$, with a homogeneous Dirichlet boundary condition everywhere on $\partial\omega_{\mathbf{a}}\setminus\Gamma_{\mathrm{N}}$. Then, (3.24) is further equivalent to finding $s_h^{\mathbf{a}}\in V_{h,\mathrm{D}}^{\mathbf{a}}$ such that

$$(\nabla s_h^{\mathbf{a}}, \nabla v_h) = (\nabla(\psi_{\mathbf{a}}u_h), \nabla v_h) \qquad \forall v_h\in V_h^{\mathbf{a}}.$$

3.4 Local efficiency

In this section, we extend the polynomial-degree-robust, local error lower bound from [18, Theorem 3.17] to inhomogeneous boundary conditions and variable polynomial degree. Define the spaces

$$H_*^1(\omega_{\mathbf{a}}) := \{v\in H^1(\omega_{\mathbf{a}});\ (v,1)_{\omega_{\mathbf{a}}} = 0\}, \qquad \mathbf{a}\in\mathcal{V}_h\setminus\mathcal{V}_h^{\mathrm{ext,D}}, \tag{3.25a}$$

$$H_*^1(\omega_{\mathbf{a}}) := \{v\in H^1(\omega_{\mathbf{a}});\ v = 0 \text{ on } \partial\omega_{\mathbf{a}}\cap\partial\Gamma_{\mathrm{D}}\}, \qquad \mathbf{a}\in\mathcal{V}_h^{\mathrm{ext,D}}. \tag{3.25b}$$

Then, the Poincaré–Friedrichs inequality states that

$$\|v\|_{\omega_{\mathbf{a}}} \le C_{\mathrm{PF},\omega_{\mathbf{a}}}h_{\omega_{\mathbf{a}}}\|\nabla v\|_{\omega_{\mathbf{a}}} \qquad \forall v\in H_*^1(\omega_{\mathbf{a}}),$$

cf. Veeser and Verfürth [30] and the references therein. Similarly, the broken Poincaré–Friedrichs inequality states that

$$\|v\|_{\omega_{\mathbf{a}}} \leq C_{\mathrm{bPF},\omega_{\mathbf{a}}} h_{\omega_{\mathbf{a}}} \left(\|\nabla v\|_{\omega_{\mathbf{a}}} + \left\{ \sum_{e \in \mathcal{E}_h^{\mathrm{int}} \cup \mathcal{E}_h^{\mathrm{ext,D}},\, \mathbf{a} \in \mathcal{V}_e} h_e^{-1} \|\Pi_e^0 [\![v]\!]\|_e^2 \right\}^{1/2} \right), \tag{3.26}$$

for any $v \in H^1(\mathcal{T}_h)$, with $(v,1)_{\omega_{\mathbf{a}}} = 0$ when $\mathbf{a} \in \mathcal{V}_h \setminus \mathcal{V}_h^{\mathrm{ext,D}}$, see Brenner [4, Remark 1.1] and the references therein. Define $C_{\mathrm{cont,PF}} := \max_{\mathbf{a} \in \mathcal{V}_h} \{1 + C_{\mathrm{PF},\omega_{\mathbf{a}}} h_{\omega_{\mathbf{a}}} \|\nabla \psi_{\mathbf{a}}\|_{\infty,\omega_{\mathbf{a}}}\}$ and $C_{\mathrm{cont,bPF}} := \max_{\mathbf{a} \in \mathcal{V}_h} \{1 + C_{\mathrm{bPF},\omega_{\mathbf{a}}} h_{\omega_{\mathbf{a}}} \|\nabla \psi_{\mathbf{a}}\|_{\infty,\omega_{\mathbf{a}}}\}$. The constants $C_{\mathrm{cont,PF}}$ and $C_{\mathrm{cont,bPF}}$ only depend on the mesh regularity parameter $\kappa_{\mathcal{T}}$ and can be fully estimated from above, see the discussion in [18, proofs of Lemmas 3.12 and 3.13 and Section 4.3.2].

To state our local efficiency result, we introduce some assumptions. First, we link the discrete gradient $\mathfrak{G}(u_h)$ to the broken gradient ∇u_h and the jumps in u_h via

$$\mathfrak{G}(u_h) = \nabla u_h - \vartheta \sum_{e \in \mathcal{E}_h} \mathfrak{l}_e([\![u_h]\!]), \tag{3.27}$$

where $\vartheta \in \{-1, 0, 1\}$ is a parameter (cf. (4.1) below), and the lifting operator $\mathfrak{l}_e : L^2(e) \to [\mathbb{P}_0(\mathcal{T}_e)]^2$ is such that, cf. [12, Section 4.3],

$$(\mathfrak{l}_e([\![u_h]\!]), \mathbf{v}_h)_{\mathcal{T}_e} = \langle \{\!\{\mathbf{v}_h\}\!\} \cdot \mathbf{n}_e, [\![u_h]\!] \rangle_e \qquad \forall \mathbf{v}_h \in [\mathbb{P}_0(\mathcal{T}_e)]^2, \tag{3.28}$$

where $\mathcal{T}_e$ denotes the triangles sharing the edge e. Moreover, we assume that u_h and $\mathfrak{G}(u_h)$ are piecewise polynomials. More precisely, we introduce the set of integer numbers $\mathsf{p} := \{p_K \in \mathbb{N},\ K \in \mathcal{T}_h\}$, and we define the following spaces:

$$S_{h,\mathsf{p}} := \{v_h \in H^1(\mathcal{T}_h);\ v_h|_K \in \mathbb{P}_{p_K}(K)\ \forall K \in \mathcal{T}_h\}, \tag{3.29a}$$

$$S_{h,\mathsf{p}-1} := \{v_h \in H^1(\mathcal{T}_h);\ v_h|_K \in \mathbb{P}_{p_K-1}(K)\ \forall K \in \mathcal{T}_h\}. \tag{3.29b}$$

Then, we assume that

$$u_h \in S_{h,\mathsf{p}}, \qquad \mathfrak{G}(u_h) \in [S_{h,\mathsf{p}-1}]^2, \tag{3.30}$$

and that the polynomial degrees assigned to vertices are such that

$$p_{\mathbf{a}} := \max_{K \in \mathcal{T}_{\mathbf{a}}} p_K, \qquad \forall \mathbf{a} \in \mathcal{V}_h. \tag{3.31}$$

Theorem 3.11 (Polynomial-degree-robust local efficiency for varying polynomial degree and inhomogeneous boundary conditions)**.** *Let u be the weak solution of (2.2), let $u_h \in S_{h,\mathsf{p}}$ and $\mathfrak{G}(u_h) \in [S_{h,\mathsf{p}-1}]^2$. Assume (3.31) for the polynomial degrees and that the local hat function orthogonality (3.6) holds. Consider Definition 3.5 of $\boldsymbol{\sigma}_h$. Then, for all $K \in \mathcal{T}_h$, with the constant C_{st} of [18, inequality (3.40)] only depending on $\kappa_{\mathcal{T}}$, the following holds:*

$$\|\mathfrak{G}(u_h) + \boldsymbol{\sigma}_h\|_K \leq C_{\mathrm{st}} C_{\mathrm{cont,PF}} \sum_{\mathbf{a} \in \mathcal{V}_K} \|\nabla u - \mathfrak{G}(u_h)\|_{\omega_{\mathbf{a}}} \tag{3.32a}$$

$$+ C_{\mathrm{st}} \sum_{\mathbf{a} \in \mathcal{V}_K} \left\{ \sum_{K' \in \mathcal{T}_{\mathbf{a}}} \left(\frac{h_{K'}}{\pi} \|\psi_{\mathbf{a}} f - \Pi_{Q_h(\omega_{\mathbf{a}})}(\psi_{\mathbf{a}} f)\|_{K'} \right)^2 \right\}^{1/2} + \Delta_{\mathrm{N}},$$

with the oscillation of the inhomogeneous Neumann condition given by

$$\Delta_{\mathrm{N}} := C_{\mathrm{st}} \sum_{\mathbf{a}\in\mathcal{V}_K} \left\{ \sum_{K'\in\mathcal{T}_{\mathbf{a}}} \left\{ \sum_{e\in\mathcal{E}_K^{\mathrm{N}}} \left(C_{\mathrm{t},K,e} h_e^{1/2} \|\psi_{\mathbf{a}}\sigma_{\mathrm{N}} - \tilde{g}_{\mathrm{N}}^{\mathbf{a}}\|_e \right) \right\}^2 \right\}^{1/2}, \tag{3.32b}$$

where $\tilde{g}_{\mathrm{N}}^{\mathbf{a}} = \Pi_{\mathbf{V}_h(\omega_{\mathbf{a}})\cdot\mathbf{n}}(\psi_{\mathbf{a}}\sigma_{\mathrm{N}})$. *Consider now Definition 3.8 of* s_h *and assume (3.27). Then, for all* $K \in \mathcal{T}_h$, *with the constant* C *only depending on* $\kappa_{\mathcal{T}}$, *see [18, Section 4.3.2], and* $\mathcal{E}_K^+ := \{e \in \mathcal{E}_h^{\mathrm{int}} \cup \mathcal{E}_h^{\mathrm{ext,D}} | \exists \mathbf{a} \in \mathcal{V}_K, \exists K' \in \mathcal{T}_{\mathbf{a}}, e \in \mathcal{E}_{K'}\}$, *the following holds:*

$$\begin{aligned} \|\mathfrak{G}(u_h) - \nabla s_h\|_K \le C_{\mathrm{st}} C_{\mathrm{cont,bPF}} \sum_{\mathbf{a}\in\mathcal{V}_K} \|\nabla u - \mathfrak{G}(u_h)\|_{\omega_{\mathbf{a}}} \\ + C \left\{ \sum_{e\in\mathcal{E}_K^+} h_e^{-1} \|\Pi_e^0 [\![u - u_h]\!]\|_e^2 \right\}^{1/2} + \Delta_{\mathrm{D}}, \end{aligned} \tag{3.33a}$$

with the oscillation of the inhomogeneous Dirichlet condition given by

$$\Delta_{\mathrm{D}} := C_{\mathrm{st}} \sum_{\mathbf{a}\in\mathcal{V}_K} \left\{ \sum_{K'\in\mathcal{T}_{\mathbf{a}}} \left\{ \sum_{e\in\mathcal{E}_K^{\mathrm{D}}} \left(C_{\mathrm{t},K,e} h_e^{1/2} \|\nabla(\psi_{\mathbf{a}} u_{\mathrm{D}})\cdot\mathbf{t}_\Omega - \tilde{g}_{\mathrm{D}}^{\mathbf{a}}\|_e \right) \right\}^2 \right\}^{1/2}, \tag{3.33b}$$

where $\tilde{g}_{\mathrm{D}}^{\mathbf{a}} = \Pi_{\mathbf{V}_h(\omega_{\mathbf{a}})\cdot\mathbf{n}}(\nabla(\psi_{\mathbf{a}} u_{\mathrm{D}})\cdot\mathbf{t}_\Omega)$.

Proof. Let $K \in \mathcal{T}_h$. Using the partition of unity as in [18, Theorem 3.17], it suffices, for all $\mathbf{a} \in \mathcal{V}_K$, to bound $\|\psi_{\mathbf{a}}\mathfrak{G}(u_h) + \boldsymbol{\varsigma}_h^{\mathbf{a}}\|_{\omega_{\mathbf{a}}}$ with $\boldsymbol{\varsigma}_h^{\mathbf{a}}$ given by (3.7) for the flux reconstruction. Similarly, for the potential reconstruction, it is enough to bound $\|\mathrm{R}_{\frac{\pi}{2}}\nabla(\psi_{\mathbf{a}} u_h) + \boldsymbol{\varsigma}_h^{\mathbf{a}}\|$ with $\boldsymbol{\varsigma}_h^{\mathbf{a}}$ given by (3.15).

For interior vertices $\mathbf{a} \in \mathcal{V}_h^{\mathrm{int}}$, the assertion coincides with that of [18, Theorem 3.17]. Indeed, the polynomial degree of the reconstructions $\boldsymbol{\sigma}_h$ and s_h is fixed by $p_{\mathbf{a}}$ on the patch $\mathcal{T}_{\mathbf{a}}$ so that the conditions (3.41) and (3.43) of [18] hold, whereas the contributions on boundary edges $e \in \mathcal{E}_K^{\mathrm{N}}$ and $e \in \mathcal{E}_K^{\mathrm{D}}$ in (3.32a) and (3.33a), respectively, are discarded by the hat function $\psi_{\mathbf{a}}$.

For boundary vertices $\mathbf{a} \in \mathcal{V}_h^{\mathrm{ext}}$, we first treat the inhomogeneous Neumann boundary condition imposed on the spaces $\mathbf{V}_{h,\mathrm{N}}^{\mathbf{a}}$ in (3.9a). First, the continuous-level problem of [18, Lemma 3.12] will appear with an inhomogeneous Neumann boundary condition $g_{\mathrm{N}}^{\mathbf{a}} := \psi_{\mathbf{a}}\sigma_{\mathrm{N}}$ on $\partial\omega_{\mathbf{a}} \cap \Gamma_{\mathrm{N}}$, with $r_{\mathbf{a}}$ in the space $H_*^1(\omega_{\mathbf{a}})$ of (3.25) satisfying

$$(\nabla r_{\mathbf{a}}, \nabla v)_{\omega_{\mathbf{a}}} = -(\boldsymbol{\tau}_h^{\mathbf{a}}, \nabla v)_{\omega_{\mathbf{a}}} + (g^{\mathbf{a}}, v)_{\omega_{\mathbf{a}}} - \langle g_{\mathrm{N}}^{\mathbf{a}}, v\rangle_{\partial\omega_{\mathbf{a}}\cap\Gamma_{\mathrm{N}}} \qquad \forall v \in H_*^1(\omega_{\mathbf{a}}), \tag{3.34}$$

where $\boldsymbol{\tau}_h^{\mathbf{a}} := \psi_{\mathbf{a}}\mathfrak{G}(u_h)$ and $g^{\mathbf{a}} := \psi_{\mathbf{a}} f - \nabla\psi_{\mathbf{a}}\cdot\mathfrak{G}(u_h)$. Proceeding as in [18, Lemma 3.12], we obtain $\|\nabla r_{\mathbf{a}}\|_{\omega_{\mathbf{a}}} \le C_{\mathrm{cont,PF}}\|\nabla u - \mathfrak{G}(u_h)\|_{\omega_{\mathbf{a}}}$. The local discrete formulation (3.7) leads us to the problem: find $\tilde{r}_{\mathbf{a}} \in H_*^1(\omega_{\mathbf{a}})$ such that

$$(\nabla \tilde{r}_{\mathbf{a}}, \nabla v)_{\omega_{\mathbf{a}}} = -(\boldsymbol{\tau}_h^{\mathbf{a}}, \nabla v)_{\omega_{\mathbf{a}}} + (\tilde{g}^{\mathbf{a}}, v)_{\omega_{\mathbf{a}}} - \langle \tilde{g}_{\mathrm{N}}^{\mathbf{a}}, v\rangle_{\partial\omega_{\mathbf{a}}\cap\Gamma_{\mathrm{N}}} \qquad \forall v \in H_*^1(\omega_{\mathbf{a}}),$$

which is a modification of (3.34) with polynomial source term $\tilde{g}^{\mathbf{a}} := \Pi_{Q_h(\omega_{\mathbf{a}})}(\psi_{\mathbf{a}} f) - \nabla\psi_{\mathbf{a}}\cdot\mathfrak{G}(u_h)$ and polynomial Neumann term $\tilde{g}_{\mathrm{N}}^{\mathbf{a}} = \Pi_{\mathbf{V}_h(\omega_{\mathbf{a}})\cdot\mathbf{n}}(\psi_{\mathbf{a}}\sigma_{\mathrm{N}})$. Then, bounding the misfit $\sup_{v\in H_*^1(\omega_{\mathbf{a}});\, \|\nabla v\|_{\omega_{\mathbf{a}}}=1} \langle g_{\mathrm{N}}^{\mathbf{a}} - \tilde{g}_{\mathrm{N}}^{\mathbf{a}}, v\rangle_{\partial\omega_{\mathbf{a}}\cap\Gamma_{\mathrm{N}}}$ as in the proof of Theorem 3.3, we

arrive at

$$\|\nabla\tilde{r}_{\mathbf{a}}\|_{\omega_{\mathbf{a}}} \le C_{\mathrm{cont,PF}}\|\nabla u - \mathfrak{G}(u_h)\|_{\omega_{\mathbf{a}}} + \left\{\sum_{K'\in\mathcal{T}_{\mathbf{a}}}\Big(\frac{h_{K'}}{\pi}\|\psi_{\mathbf{a}}f - \Pi_{Q_h(\omega_{\mathbf{a}})}(\psi_{\mathbf{a}}f)\|_{K'}\Big)^2\right\}^{1/2} + \left\{\sum_{K'\in\mathcal{T}_{\mathbf{a}}}\left\{\sum_{e\in\mathcal{E}_K^{\mathrm{N}}}\Big(C_{\mathrm{t},K,e}h_e^{1/2}\|\psi_{\mathbf{a}}\sigma_{\mathrm{N}} - \tilde{g}_{\mathrm{N}}^{\mathbf{a}}\|_e\Big)\right\}^2\right\}^{1/2}.$$

Finally, the stability result in [2, Theorem 7], based on [8, Corollary 3.4] and [9, Theorem 7.1], gives $\|\psi_{\mathbf{a}}\mathfrak{G}(u_h) + \boldsymbol{\varsigma}_h^{\mathbf{a}}\|_{\omega_{\mathbf{a}}} \le C_{\mathrm{st}}\|\nabla\tilde{r}_{\mathbf{a}}\|_{\omega_{\mathbf{a}}}$, and (3.32a) follows.

We now treat the inhomogeneous Neumann boundary condition on $\partial\omega_{\mathbf{a}}\cap\Gamma_{\mathrm{D}}$ dictated by (3.17) (note that the Dirichlet boundary condition on Γ_{D} appears here as a Neumann boundary condition on $\partial\omega_{\mathbf{a}}\cap\Gamma_{\mathrm{D}}$). Similarly to [18, Lemma 3.13], we introduce the problem: find $r_{\mathbf{a}}\in H^1_\flat(\mathcal{T}_{\mathbf{a}})$ such that

$$(\nabla r_{\mathbf{a}},\nabla v)_{\omega_{\mathbf{a}}} = -(\boldsymbol{\tau}_h^{\mathbf{a}},\nabla v)_{\omega_{\mathbf{a}}} + (g^{\mathbf{a}},v)_{\omega_{\mathbf{a}}} - \langle g_{\mathrm{D}}^{\mathbf{a}},v\rangle_{\partial\omega_{\mathbf{a}}\cap\Gamma_{\mathrm{D}}} \qquad \forall v\in H^1_\flat(\mathcal{T}_{\mathbf{a}}),$$

with $g_{\mathrm{D}}^{\mathbf{a}} := \nabla(\psi_{\mathbf{a}}u_{\mathrm{D}})\cdot\mathbf{t}_\Omega$, $\boldsymbol{\tau}_h^{\mathbf{a}} := \mathrm{R}_{\frac{\pi}{2}}\nabla(\psi_{\mathbf{a}}u_h)$, and $g^{\mathbf{a}} := 0$, and with

$$H^1_\flat(\mathcal{T}_{\mathbf{a}}) := \{v\in H^1(\omega_{\mathbf{a}});\ (v,1)_{\omega_{\mathbf{a}}} = 0\}, \qquad \mathbf{a}\in\mathcal{V}_h^{\mathrm{ext}}\setminus\mathcal{V}_h^{\mathrm{ext,N}},$$
$$H^1_\flat(\mathcal{T}_{\mathbf{a}}) := \{v\in H^1(\omega_{\mathbf{a}});\ v = 0 \text{ on } \partial\omega_{\mathbf{a}}\cap\Gamma_{\mathrm{N}}\}, \qquad \mathbf{a}\in\mathcal{V}_h^{\mathrm{ext,N}}.$$

Again, the local discrete formulation (3.15) leads us to study the above problem with a polynomial Neumann term given by $\tilde{g}_{\mathrm{D}}^{\mathbf{a}}=\Pi_{\mathbf{V}_h(\omega_{\mathbf{a}})\cdot\mathbf{n}}(\nabla(\psi_{\mathbf{a}}u_{\mathrm{D}})\cdot\mathbf{t}_\Omega)$, and we have to bound the misfit $\sup_{v\in H^1_\flat(\mathcal{T}_{\mathbf{a}});\,\|\nabla v\|_{\omega_{\mathbf{a}}}=1}\langle g_{\mathrm{D}}^{\mathbf{a}} - \tilde{g}_{\mathrm{D}}^{\mathbf{a}},v\rangle_{\partial\omega_{\mathbf{a}}\cap\Gamma_{\mathrm{D}}}$. Using (3.26) and proceeding as in [18, Section 4.3.2], we obtain

$$\|\nabla\tilde{r}_{\mathbf{a}}\|_{\omega_{\mathbf{a}}} \le C_{\mathrm{cont,bPF}}\left(\|\nabla(u-u_h)\|_{\omega_{\mathbf{a}}} + \left\{\sum_{e\in\mathcal{E}_h^{\mathrm{int}}\cup\mathcal{E}_h^{\mathrm{ext,D}},\,\mathbf{a}\in\mathcal{V}_e} h_e^{-1}\|\Pi_e^0[\![u-u_h]\!]\|_e^2\right\}^{1/2}\right) + \left\{\sum_{K'\in\mathcal{T}_{\mathbf{a}}}\left\{\sum_{e\in\mathcal{E}_K^{\mathrm{D}}}\Big(C_{\mathrm{t},K,e}h_e^{1/2}\|\nabla(\psi_{\mathbf{a}}u_{\mathrm{D}})\cdot\mathbf{t}_\Omega - \tilde{g}_{\mathrm{D}}^{\mathbf{a}}\|_e\Big)\right\}^2\right\}^{1/2},$$

whereas [2, Theorem 7] again implies $\|\mathrm{R}_{\frac{\pi}{2}}\nabla(\psi_{\mathbf{a}}u_h) + \boldsymbol{\varsigma}_h^{\mathbf{a}}\|_{\omega_{\mathbf{a}}} \le C_{\mathrm{st}}\|\nabla\tilde{r}_{\mathbf{a}}\|_{\omega_{\mathbf{a}}}$. Finally, employing (3.27) allows us to conclude that (3.33a) holds, as in [18, Section 4.3.2]. □

4 The hp-adaptive strategy

We present in this section our hp-refinement strategy driven by the equilibrated flux a posteriori error estimates devised in Section 3. We also briefly discuss the implementation of the mixed finite element solves for the flux and potential reconstructions. Even though our strategy is generic as the estimates of Section 3, we prefer to present it on a discontinuous Galerkin discretization to fix ideas.

4.1 Discretization by the interior penalty discontinuous Galerkin method

Consider the interior penalty discontinuous Galerkin method: find $u_h \in S_{h,\mathsf{p}}$ (defined by (3.29a)) such that

$$\sum_{K\in\mathcal{T}_h} (\nabla u_h, \nabla v_h)_K - \sum_{e\in\mathcal{E}_h^{\mathrm{int}}\cup\mathcal{E}_h^{\mathrm{ext,D}}} \{\langle \{\!\{\nabla u_h\}\!\}\cdot\mathbf{n}_e, [\![v_h]\!]\rangle_e + \vartheta\langle \{\!\{\nabla v_h\}\!\}\cdot\mathbf{n}_e, [\![u_h-u]\!]\rangle_e\}$$
$$+ \sum_{e\in\mathcal{E}_h^{\mathrm{int}}\cup\mathcal{E}_h^{\mathrm{ext,D}}} \langle \alpha h_e^{-1}[\![u_h-u]\!], [\![v_h]\!]\rangle_e = (f,v_h) - \langle \sigma_{\mathrm{N}}, v_h\rangle_{\Gamma_{\mathrm{N}}} \quad \forall v_h \in S_{h,\mathsf{p}}, \tag{4.1}$$

where α is a positive penalty parameter and $\vartheta \in \{-1,0,1\}$ corresponds respectively to the nonsymmetric (NIPG), incomplete (IIPG), and symmetric (SIPG) versions of the method; ϑ is the parameter considered in (3.27). Remark that above, $[\![u_h-u]\!] = [\![u_h]\!]$ for $e \in \mathcal{E}_h^{\mathrm{int}}$ and $[\![u_h-u]\!] = [\![u_h-u_{\mathrm{D}}]\!]$ for $e \in \mathcal{E}_h^{\mathrm{ext,D}}$. Taking $\psi_{\mathbf{a}} \in S_{h,\mathsf{p}}$ as the test function in (4.1) for the vertices $\mathbf{a} \in \mathcal{V}_h \setminus \mathcal{V}_h^{\mathrm{ext,D}}$ and using the definition (3.27) of the discrete gradient, we infer the hat-function orthogonality condition (3.6).

An important issue with interior penalty discontinuous Galerkin methods is the choice of the penalty parameter α. Typical choices, supported theoretically and numerically, are $\alpha = O(p^2)$ for the symmetric variant and a p-independent choice $\alpha > 0$ for the nonsymmetric one. Numerical evidence indicates that a p-independent choice for α is also possible for the incomplete version.

4.2 Smoothness indicator

Let η_K, $K \in \mathcal{T}_h$ be the local error indicators of (3.4b). Let $\Pi_{S_{h,\mathsf{p}-1}}(u_h)$ be the $L^2(\Omega)$-orthogonal projection of u_h onto the lower-polynomial-degree space $S_{h,\mathsf{p}-1}$ defined by (3.29b); note that this projection can be evaluated elementwise and that its actual computation is particularly simple if local hierarchical polynomials bases of $S_{h,\mathsf{p}}$ are considered. Then, we also evaluate the local error indicators from $\Pi_{S_{h,\mathsf{p}-1}}(u_h)$, and we denote the corresponding values by $\eta_K^{\mathsf{p}-1}$ for all $K \in \mathcal{T}_h$. Obviously, $\Pi_{S_{h,\mathsf{p}-1}}(u_h)$ does not satisfy the hat-function orthogonality (3.6). However, $\eta_K^{\mathsf{p}-1}$ is not used for an error estimate but only for the smoothness indicator.

We define the following local smoothness indicator:

$$g_K := \frac{\eta_K}{\eta_K^{\mathsf{p}-1}} \qquad \forall K \in \mathcal{T}_h. \tag{4.2}$$

Assume that the local smoothness of the exact solution can be quantified by the real number $r_K \geq 1$ such that $u|_K \in H^{r_K}(K)$. Then, finite element approximation theory indicates that $g_K = O(h_K^\beta)$ with $\beta = 1$ if $p_K + 1 \leq r_K$, $\beta \in (0,1)$ if $r_K \in (p_K, p_K+1)$, and $\beta = 0$ if $r_K \leq p_K$. We expect that if $u \in H^{r_K}(K)$, then the optimal local polynomial degree p_K satisfies

$$p_K \leq r_K \leq p_K + 1. \tag{4.3}$$

We define the limit values

$$G_K^{\mathrm{L}} := h_K^{1/2}, \qquad G_K^{\mathrm{U}} := h_K^{-1/2}. \tag{4.4}$$

Assuming without loss of generality that $h_K \leq 1$, we observe that $G_K^{\mathrm{L}} \leq 1 \leq G_K^{\mathrm{U}}$. This leads us to the following heuristics:

- If $g_K \le G_K^{\mathrm{L}}$, we expect that $p_K + 1 \le r_K$, and we should increase p_K.
- If $g_K \ge G_K^{\mathrm{U}}$, we expect that $r_K \le p_K$, and we should decrease p_K.
- If $G_K^{\mathrm{L}} < g_K < G_K^{\mathrm{U}}$, we keep p_K unmodified.

Let us notice that in practical computations, the case where $g_K \ge G_K^{\mathrm{U}}$ seldom appears.

4.3 hp-adaptation algorithms

Let $\varpi > 0$ be a given error tolerance. Our aim is to adapt the mesh and the polynomial degrees in order to satisfy the condition

$$\eta \le \varpi, \tag{4.5}$$

where η is the global error indicator. In order to fulfil (4.5), we simply require that

$$\eta_K \le \varpi_K := \frac{\varpi}{\sqrt{\#\mathcal{T}_h}} \qquad \forall K \in \mathcal{T}_h, \tag{4.6}$$

where $\#\mathcal{T}_h$ denotes the number of elements in the mesh. The equidistribution condition (4.6) is stronger than (4.5); its advantage is that all elements can be adapted at once without any sorting. In practice, we actually set $\varpi_K := c_F \varpi/\sqrt{\#\mathcal{T}_h}$ where $c_F = 1/2$ is a safety factor.

We first introduce a simple Algorithm 1 consisting only of refinements, that is, either the polynomial degree is increased, or the mesh size is halved locally.

Algorithm 1 Simple hp-adaptive algorithm

```
let u_h ∈ S_{h,p} and ϖ > 0 be given
for all K ∈ T_h do
  let h_K = diam(K) and let p_K be the corresponding polynomial degree
  compute η_K as in Theorem 3.3, g_K by (4.2), and ϖ_K by (4.6)
  if η_K > ϖ_K then
    if g_K < G_K^L then
      p_K^new := p_K + 1;  ρ := 1                    (p-refinement)
    else
      p_K^new := p_K;      ρ := 2                    (h-refinement)
    end if
  end if
  h_K^new := h_K/ρ
end for
```

A more computationally-effective Algorithm 2, also allows for decreasing the polynomial degree or for local coarsening of the mesh. The modification of the local mesh size is driven by the criterion

$$h_K^{\mathrm{new}} := h_K/\rho, \qquad \rho := c_F \left(\eta_K/\varpi_K\right)^{1/p_K}, \tag{4.7}$$

where $c_F = 1.25$ is again a safety factor. This formula is motivated by the relations $\eta_K \approx c h_K^{p_K}$ and $\varpi_K \approx c(h_K^{\mathrm{new}})^{p_K}$, from which we can eliminate the unknown constant c. In order to avoid a strong refinement, we additionally restrict $\rho \le 2$. Moreover, if the local error indicator η_K is several times smaller (in our computations ten times

smaller) than the local tolerance ϖ_K, we carry out a coarsening using again (4.7) evaluated with p_K^{new}.

Algorithm 2 Full hp-adaptive algorithm

let $u_h \in S_{h,\mathsf{p}}$ and $\varpi > 0$ be given
for all $K \in \mathcal{T}_h$ **do**
  let $h_K = \mathrm{diam}(K)$ and let p_K be the corresponding polynomial degree
  compute η_K as in Theorem 3.3, g_K by (4.2), and ϖ_K by (4.6)
  if $\eta_K > \varpi_K$ **then**
    if $g_K < G_K^{\mathrm{L}}$ **then**
      $p_K^{\mathrm{new}} := p_K + 1; \qquad \rho := 1$ (p-refinement)
    else
      $p_K^{\mathrm{new}} := p_K; \qquad \rho := (\eta_K/\varpi_K)^{1/p_K}$ (h-refinement)
    end if
  else if $\eta_K < \varpi_K/10$ **then**
    if $g_K < G_K^{\mathrm{L}}$ **then**
      $p_K^{\mathrm{new}} := p_K + 1; \quad \rho := (\eta_K/\varpi_K)^{1/(p_K+1)}$ (h-modification & p-refinement)
    else if $G_K^{\mathrm{L}} \le g_K \le G_K^{\mathrm{U}}$ **then**
      $p_K^{\mathrm{new}} := p_K; \qquad \rho := (\eta_K/\varpi_K)^{1/p_K}$ (h-modification)
    else if $G_K^{\mathrm{U}} \le g_K$ **then**
      $p_K^{\mathrm{new}} := p_K - 1; \quad \rho := (\eta_K/\varpi_K)^{1/(p_K-1)}$ (h-modification & p-derefinement)
    end if
  end if
  $h_K^{\mathrm{new}} := h_K/\min(\rho, 2)$
end for

Algorithms 1 and 2 define for each $K \in \mathcal{T}_h$ new values h_K^{new} and p_K^{new}. Consequently, we generate a new mesh $\mathcal{T}_h^{\mathrm{new}}$ which consists of isotropic triangles. The length of edges of each $K' \in \mathcal{T}_h^{\mathrm{new}}$ should be approximately equal to h_K^{new}, where $K \in \mathcal{T}_h$ is the closest triangle to $K' \in \mathcal{T}_h^{\mathrm{new}}$. In practice, for the barycentre of each $K \in \mathcal{T}_h$, we define an isotropic Riemann metric (the Euclidean metric scaled by $1/h_K^{\mathrm{new}}$). Then, with the aid of the code ANGENER [14], we create $\mathcal{T}_h^{\mathrm{new}}$, see [13, 15] for more details. The elementwise constants p_K^{new}, $K \in \mathcal{T}_h$, are then interpolated onto $\mathcal{T}_h^{\mathrm{new}}$.

4.4 Implementation of the mixed finite element solves

The patchwise mixed finite element problems (3.7) and (3.15) are solved using the Schur complement and a direct solver. An important issue when the polynomial degree grows is the choice of basis functions so as to tame the growth of the condition number of the corresponding mass matrices. Starting with the usual shape functions that constitute the dual basis of the canonical degrees of freedom of the Raviart–Thomas finite element, significant improvements in the condition number of the mass matrix are observed if a Gram–Schmidt process is applied to orthogonalize the shape functions attached to cell-based degrees of freedom. A further marginal reduction of the condition number is achieved if suitable linear combinations are formed to

p	original	cell orth.	cell and face orth.
1	2.24E+01	2.77E+01	3.60E+01
2	1.78E+02	1.09E+02	1.07E+02
3	4.74E+03	2.44E+02	2.02E+02
4	1.42E+05	5.41E+02	3.93E+02
5	4.66E+06	1.10E+03	6.24E+02
6	1.46E+08	2.34E+03	9.63E+02
7	4.43E+09	5.18E+03	1.16E+03

Tab. 1: Mass matrix condition number for the local mixed finite element problems with various choices of the basis functions as a function of polynomial degree p, generic shape-regular patch

orthogonalize cell- and face-based shape functions. Elemental results are presented in Table 1.

5 Numerical examples

In this section we first check the behavior of the derived estimates for a smooth solution. We then study the computational performance of the hp-adaptive Algorithms 1 and 2 producing a sequence of non-nested unstructured hp-grids for three singular benchmark solutions from [23]. In each case, we consider the problem (2.1) with $\Gamma_{\mathrm{D}} = \partial\Omega$. The right-hand side f and the Dirichlet datum u_D are evaluated from the known exact solution.

5.1 A smooth solution

We first consider $\Omega = (0,1) \times (0,1)$ and $u(x_1, x_2) = \sin(2\pi x_1)\sin(2\pi x_2)$. Here a given sequence of four unstructured non-nested grids is considered, with SIPG and NIPG (4.1) methods and polynomial approximations up to order 6 (similar results on uniformly refined nested grids in the IIPG case were already presented in [18, Section 5]). The penalty parameter α was chosen $\alpha = 5p^2$ for SIPG and $\alpha = 1$ for NIPG. The results are presented in Tables 2–3, where $\|u-u_h\|_{\mathrm{J}}^2 := \sum_{e\in\mathcal{E}_h} h_e^{-1}\|\Pi_e^0[\![u-u_h]\!]\|_e^2$ is the jump seminorm and $\|u-u_h\|_{\mathrm{DG}}^2 := \|\nabla u - \mathfrak{G}(u_h)\|^2 + \|u-u_h\|_{\mathrm{J}}^2$ is the DG norm. The estimator η and its components are given by Theorem 3.3; the full DG estimator is $\eta_{\mathrm{DG}}^2 := \eta^2 + \|u-u_h\|_{\mathrm{J}}^2$. The tables also report the effectivity indices $I^{\mathrm{eff}} := \frac{\eta}{\|\nabla(u-u_h)\|}$ and $I_{\mathrm{DG}}^{\mathrm{eff}} := \frac{\eta_{\mathrm{DG}}}{\|u-u_h\|_{\mathrm{DG}}}$. Asymptotic exactness is observed in both cases, similarly to [18, Section 5].

5.2 Case 1: re-entrant corner singularity

Here $\Omega := (-1,1)^2 \setminus [0,1]^2$ and

$$u(r,\varphi) = r^{2/3}\sin(2\varphi/3), \tag{5.1}$$

where (r,φ) are the polar coordinates. In this case $f = 0$. Owing to the re-entrant corner, this problem features a singularity at the origin such that $u \in H^{5/3-\epsilon}(\Omega)$, $\forall\epsilon > 0$. Henceforth, we consider the incomplete version ($\vartheta = 0$) with $\alpha = 20$; note that $\|\nabla u - \mathfrak{G}(u_h)\| = \|\nabla(u-u_h)\|$ in this case, cf. (3.27). The presence of the singularity does not allow faster convergence than $O(h^{2/3})$ for uniformly refined grids.

h	p	$\|\nabla u - \mathfrak{G}(u_h)\|$	$\|u-u_h\|_{\mathrm{J}}$	$\|u-u_h\|_{\mathrm{DG}}$	η_{CR}	η_{osc}	η_{NC}	η_{BC}	η	η_{DG}	I^{eff}	$I^{\mathrm{eff}}_{\mathrm{DG}}$
h_0	1	1.07E-00	1.92E-01	1.09E-00	1.12E-00	5.55E-02	4.16E-01	1.09E-09	1.25E-00	1.26E-00	1.17	1.16
$\approx h_0/2$	1	5.56E-01	7.28E-02	5.61E-01	5.71E-01	7.42E-03	1.82E-01	2.20E-10	6.07E-01	6.11E-01	1.09	1.09
$\approx h_0/4$	1	2.92E-01	2.82E-02	2.93E-01	2.96E-01	1.04E-03	8.77E-02	4.54E-11	3.10E-01	3.11E-01	1.06	1.06
$\approx h_0/8$	1	1.39E-01	9.19E-03	1.39E-01	1.40E-01	1.10E-04	3.85E-02	7.45E-12	1.45E-01	1.45E-01	1.04	1.04
h_0	2	1.54E-01	1.76E-02	1.55E-01	1.55E-01	5.10E-03	3.05E-02	1.41E-10	1.63E-01	1.64E-01	1.06	1.06
$\approx h_0/2$	2	4.07E-02	4.66E-03	4.09E-02	4.13E-02	3.53E-04	7.55E-03	2.20E-11	4.23E-02	4.26E-02	1.04	1.04
$\approx h_0/4$	2	1.10E-02	1.26E-03	1.11E-02	1.12E-02	2.51E-05	1.97E-03	2.11E-12	1.14E-02	1.15E-02	1.03	1.03
$\approx h_0/8$	2	2.50E-03	2.90E-04	2.52E-03	2.54E-03	1.30E-06	4.21E-04	1.57E-13	2.57E-03	2.59E-03	1.03	1.03
h_0	3	1.37E-02	3.96E-04	1.37E-02	1.37E-02	3.58E-04	1.74E-03	1.35E-11	1.41E-02	1.41E-02	1.03	1.03
$\approx h_0/2$	3	1.85E-03	4.53E-05	1.85E-03	1.85E-03	1.26E-05	2.10E-04	8.24E-13	1.88E-03	1.88E-03	1.01	1.01
$\approx h_0/4$	3	2.60E-04	4.79E-06	2.60E-04	2.60E-04	4.73E-07	2.54E-05	4.23E-14	2.62E-04	2.62E-04	1.01	1.01
$\approx h_0/8$	3	2.75E-05	3.75E-07	2.75E-05	2.75E-05	1.15E-08	2.55E-06	8.51E-15	2.76E-05	2.76E-05	1.01	1.01
h_0	4	9.87E-04	2.95E-05	9.87E-04	9.84E-04	2.12E-05	1.11E-04	5.61E-13	1.01E-03	1.01E-03	1.02	1.02
$\approx h_0/2$	4	6.92E-05	2.06E-06	6.93E-05	6.92E-05	3.96E-07	7.44E-06	2.09E-13	7.00E-05	7.00E-05	1.01	1.01
$\approx h_0/4$	4	5.04E-06	1.42E-07	5.04E-06	5.04E-06	7.58E-09	4.98E-07	1.36E-13	5.07E-06	5.07E-06	1.01	1.01
$\approx h_0/8$	4	2.58E-07	7.61E-09	2.59E-07	2.58E-07	8.96E-11	2.47E-08	7.63E-14	2.60E-07	2.60E-07	1.01	1.01
h_0	5	5.64E-05	6.76E-07	5.64E-05	5.63E-05	1.06E-06	4.50E-06	1.76E-12	5.75E-05	5.75E-05	1.02	1.02
$\approx h_0/2$	5	2.01E-06	2.18E-08	2.01E-06	2.01E-06	9.88E-09	1.46E-07	1.61E-12	2.03E-06	2.03E-06	1.01	1.01
$\approx h_0/4$	5	7.74E-08	6.04E-10	7.74E-08	7.73E-08	1.01E-10	4.35E-09	1.64E-12	7.76E-08	7.76E-08	1.00	1.00
$\approx h_0/8$	5	1.86E-09	1.18E-11	1.86E-09	1.86E-09	1.70E-12	1.00E-10	7.51E-13	1.86E-09	1.86E-09	1.00	1.00
h_0	6	2.85E-06	3.70E-08	2.85E-06	2.85E-06	4.70E-08	2.18E-07	3.04E-11	2.90E-06	2.90E-06	1.02	1.02
$\approx h_0/2$	6	5.42E-08	6.78E-10	5.42E-08	5.42E-08	2.40E-10	4.02E-09	3.29E-11	5.46E-08	5.46E-08	1.01	1.01
$\approx h_0/4$	6	1.07E-09	1.20E-11	1.07E-09	1.07E-09	1.03E-11	6.90E-11	2.16E-11	1.08E-09	1.08E-09	1.01	1.01

Tab. 2: Errors and estimates for a smooth solution, SIPG method

h	p	$\|\nabla u - \mathfrak{G}(u_h)\|$	$\|u-u_h\|_{\mathrm{J}}$	$\|u-u_h\|_{\mathrm{DG}}$	η_{CR}	η_{osc}	η_{NC}	η_{BC}	η	η_{DG}	I^{eff}	$I^{\mathrm{eff}}_{\mathrm{DG}}$
h_0	1	1.08E-00	1.69E-01	1.09E-00	8.05E-01	5.55E-02	7.98E-01	1.09E-09	1.17E-00	1.18E-00	1.09	1.09
$\approx h_0/2$	1	5.50E-01	7.52E-02	5.55E-01	4.18E-01	7.42E-03	3.75E-01	2.20E-10	5.66E-01	5.71E-01	1.03	1.03
$\approx h_0/4$	1	2.84E-01	3.34E-02	2.86E-01	2.18E-01	1.04E-03	1.86E-01	4.54E-11	2.87E-01	2.89E-01	1.01	1.01
$\approx h_0/8$	1	1.34E-01	1.19E-02	1.35E-01	1.04E-01	1.10E-04	8.64E-02	7.45E-12	1.36E-01	1.36E-01	1.01	1.01
h_0	2	1.65E-01	4.82E-02	1.72E-01	1.41E-01	5.10E-03	1.71E-01	1.41E-10	2.24E-01	2.30E-01	1.36	1.33
$\approx h_0/2$	2	4.28E-02	1.25E-02	4.46E-02	3.67E-02	3.53E-04	4.74E-02	2.20E-11	6.01E-02	6.14E-02	1.41	1.38
$\approx h_0/4$	2	1.14E-02	3.37E-03	1.19E-02	9.86E-03	2.51E-05	1.29E-02	2.11E-12	1.63E-02	1.66E-02	1.43	1.40
$\approx h_0/8$	2	2.58E-03	7.93E-04	2.70E-03	2.24E-03	1.30E-06	2.99E-03	1.56E-13	3.74E-03	3.82E-03	1.45	1.42
h_0	3	1.53E-02	1.25E-03	1.54E-02	1.34E-02	3.58E-04	9.19E-03	1.35E-11	1.65E-02	1.66E-02	1.08	1.08
$\approx h_0/2$	3	2.07E-03	1.66E-04	2.07E-03	1.79E-03	1.26E-05	1.22E-03	8.24E-13	2.18E-03	2.18E-03	1.05	1.05
$\approx h_0/4$	3	2.99E-04	2.00E-05	2.99E-04	2.64E-04	4.73E-07	1.59E-04	4.26E-14	3.08E-04	3.09E-04	1.03	1.03
$\approx h_0/8$	3	3.16E-05	1.68E-06	3.17E-05	2.82E-05	1.15E-08	1.60E-05	8.38E-15	3.24E-05	3.25E-05	1.02	1.02
h_0	4	1.11E-03	1.22E-04	1.12E-03	9.80E-04	2.12E-05	7.21E-04	5.19E-13	1.23E-03	1.24E-03	1.11	1.11
$\approx h_0/2$	4	7.71E-05	8.21E-06	7.75E-05	6.89E-05	3.96E-07	5.08E-05	2.27E-13	8.59E-05	8.63E-05	1.11	1.11
$\approx h_0/4$	4	5.66E-06	5.94E-07	5.69E-06	5.05E-06	7.58E-09	3.76E-06	1.38E-13	6.30E-06	6.33E-06	1.11	1.11
$\approx h_0/8$	4	2.89E-07	3.19E-08	2.91E-07	2.58E-07	8.96E-11	1.96E-07	7.45E-14	3.24E-07	3.26E-07	1.12	1.12
h_0	5	6.23E-05	3.08E-06	6.24E-05	5.62E-05	1.06E-06	3.23E-05	1.92E-12	6.57E-05	6.58E-05	1.05	1.05
$\approx h_0/2$	5	2.26E-06	1.01E-07	2.27E-06	2.04E-06	9.88E-09	1.17E-06	1.71E-12	2.36E-06	2.36E-06	1.04	1.04
$\approx h_0/4$	5	8.86E-08	3.15E-09	8.87E-08	8.17E-08	1.01E-10	3.90E-08	1.59E-12	9.06E-08	9.06E-08	1.02	1.02
$\approx h_0/8$	5	2.11E-09	6.47E-11	2.12E-09	1.96E-09	1.70E-12	9.02E-10	7.13E-13	2.16E-09	2.16E-09	1.02	1.02
h_0	6	3.18E-06	1.90E-07	3.18E-06	2.91E-06	4.70E-08	1.66E-06	2.96E-11	3.39E-06	3.39E-06	1.07	1.07
$\approx h_0/2$	6	6.00E-08	3.27E-09	6.01E-08	5.57E-08	2.40E-10	3.07E-08	2.85E-11	6.38E-08	6.39E-08	1.06	1.06
$\approx h_0/4$	6	1.20E-09	6.34E-11	1.20E-09	1.12E-09	1.03E-11	6.01E-10	2.06E-11	1.28E-09	1.28E-09	1.07	1.07

Tab. 3: Errors and estimates for a smooth solution, NIPG method

We carried out computations with $\varpi = 10^{-4}$ by both Algorithms 1 and 2. Figure 2, left, compares the convergence of the error estimator η with respect to the degrees of freedom (DoF). Figure 2, right, compares the convergence of the energy error $\|\nabla(u-u_h)\|$ and of its estimator η. We observe that Algorithm 1 leads to an exponential order of convergence. Incidentally, the experimental order of convergence is increasing here with respect to levels of adaptation (the decrease of the error is faster than any linear decrease in logarithmic scale, cf. Figure 2). The full Algorithm 2 is still more efficient due to the possibility to decrease DoF.

Table 4 shows the computational errors and the values of the various components of the error estimator η according to (3.4b). We observe that the effectivity index takes roughly constant values comprised between 1.6 and 2. Furthermore, Figure 3 shows the final hp-grids with their details obtained by both algorithms. Finally, Figure 4 shows the hp-grids with their details for selected levels of adaptation obtained by

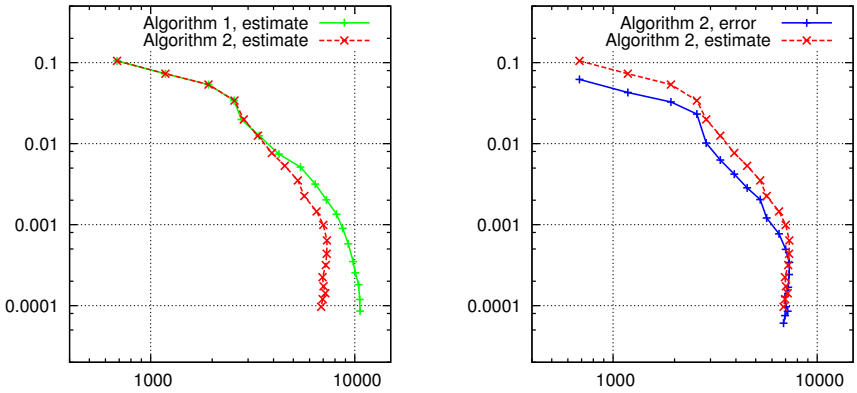

Fig. 2: Case 1, estimates η (and error $\|\nabla(u-u_h)\|$) with respect to DoF, comparison of Algorithms 1 and 2 (left) and Algorithm 2 (right)

lev	$\#\mathcal{T}_h$	DoF	$\|\nabla(u-u_h)\|$	η_{CR}	η_{osc}	η_{NC}	η_{BC}	η	I^{eff}
0	114	684	6.22E-02	6.63E-02	1.89E-15	4.48E-02	3.81E-02	1.05E-01	1.69
1	122	1180	4.28E-02	4.27E-02	1.18E-14	3.08E-02	2.92E-02	7.29E-02	1.70
2	139	1919	3.28E-02	3.37E-02	8.21E-14	2.09E-02	2.12E-02	5.36E-02	1.64
3	165	2573	2.32E-02	2.30E-02	3.88E-13	1.50E-02	1.03E-02	3.41E-02	1.47
4	174	2858	1.02E-02	1.01E-02	4.48E-13	8.22E-03	9.19E-03	1.99E-02	1.96
5	199	3351	6.27E-03	6.21E-03	1.12E-12	4.81E-03	6.18E-03	1.25E-02	2.00
6	237	3926	4.21E-03	4.23E-03	1.98E-12	3.15E-03	3.29E-03	7.66E-03	1.82
7	285	4537	2.84E-03	2.91E-03	7.47E-12	2.13E-03	2.42E-03	5.33E-03	1.88
8	338	5257	2.04E-03	2.19E-03	4.63E-11	1.45E-03	1.32E-03	3.51E-03	1.72
9	372	5658	1.21E-03	1.23E-03	1.11E-11	9.07E-04	9.99E-04	2.26E-03	1.87
10	426	6500	7.70E-04	7.69E-04	5.69E-11	5.55E-04	6.95E-04	1.46E-03	1.89
11	453	7010	4.95E-04	5.04E-04	9.77E-11	3.97E-04	4.74E-04	9.91E-04	2.00
12	469	7308	3.41E-04	3.47E-04	1.13E-10	2.55E-04	2.88E-04	6.40E-04	1.88
13	463	7286	2.42E-04	2.42E-04	1.39E-10	1.73E-04	1.94E-04	4.37E-04	1.81
14	458	7215	1.69E-04	1.69E-04	1.23E-10	1.19E-04	1.53E-04	3.17E-04	1.88
15	440	6955	1.29E-04	1.31E-04	1.45E-10	9.21E-05	9.10E-05	2.24E-04	1.73
16	435	7035	9.71E-05	9.91E-05	1.39E-10	6.89E-05	7.63E-05	1.74E-04	1.79
17	434	7167	8.52E-05	8.97E-05	1.41E-10	5.76E-05	5.47E-05	1.42E-04	1.67
18	419	6960	7.51E-05	7.97E-05	1.44E-10	5.00E-05	4.15E-05	1.21E-04	1.60
19	410	6838	6.06E-05	6.35E-05	1.47E-10	3.87E-05	3.65E-05	9.69E-05	1.60

Tab. 4: Case 1, Algorithm 2: convergence of the error and of the estimate and with its components

Algorithm 2.

5.3 Case 2: circular front

The computational domain and the exact solution are here $\Omega = (0,1)^2$ and

$$u(x_1,x_2) = \tan^{-1}(m(r-r_0)), \tag{5.2}$$

where $r = ((x_1-\bar{x}_1)^2+(x_2-\bar{x}_2)^2)^{1/2}$ and where $\bar{x}_1 = \bar{x}_2 = 0.5$, $m = 50$, and $r_0 = 0.25$. The solution has a steep wave front in the interior of the domain. Due to the $\tan^{-1}$

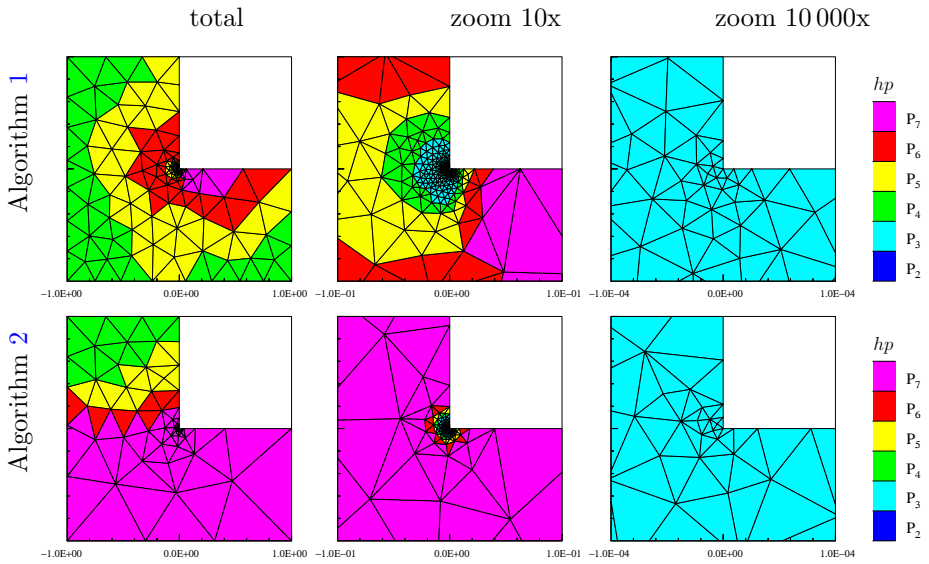

Fig. 3: Case 1, comparison of Algorithms 1 and 2: final hp-grids with details around the origin

lev	$\#\mathcal{T}_h$	DoF	$\|\nabla(u-u_h)\|$	η_{CR}	η_{osc}	η_{NC}	η_{BC}	η	I^{eff}
0	64	384	7.05E+00	5.52E+00	2.47E+01	1.77E-01	1.71E-04	2.93E+01	4.15
1	168	1040	4.91E+00	3.57E+00	9.48E+00	8.44E-02	6.33E-05	1.30E+01	2.65
2	524	3560	2.09E+00	1.87E+00	2.22E+00	3.26E-02	3.22E-06	3.98E+00	1.91
3	1370	9826	6.99E-01	6.74E-01	2.75E-01	1.26E-02	4.10E-06	9.27E-01	1.33
4	3566	25423	1.81E-01	1.81E-01	2.09E-02	3.99E-03	4.54E-06	1.99E-01	1.10
5	6746	56553	4.84E-02	4.89E-02	4.28E-03	1.26E-03	4.82E-06	5.13E-02	1.06
6	10958	96001	1.25E-02	1.26E-02	1.04E-03	3.38E-04	4.65E-06	1.30E-02	1.04
7	21876	171416	3.70E-03	3.73E-03	4.51E-04	1.07E-04	4.50E-06	3.84E-03	1.04

Tab. 5: Case 2, Algorithm 2: convergence of the error and of the estimate and with its components

function, there is also a mild singularity in the center of the circle.

We carried out computations with $\varpi = 10^{-2}$ by both algorithms. Figure 5, left, compares the convergence of the error estimator η with respect to DoF. Figure 5, right, compares the convergence of the energy error $\|\nabla(u-u_h)\|$ and of its estimator η. Here, Algorithms 1 and 2 behave similarly and yield exponential order of convergence.

Table 5 reports the energy errors and the values of the various components of the error estimator η. We observe that the effectivity index is very close to 1. Finally, Figure 6 shows the hp-grids with their details for selected levels of adaptation obtained by Algorithm 2. We observe a strong h-refinement along the steep circular front and also around the singularity at the center of the circle.

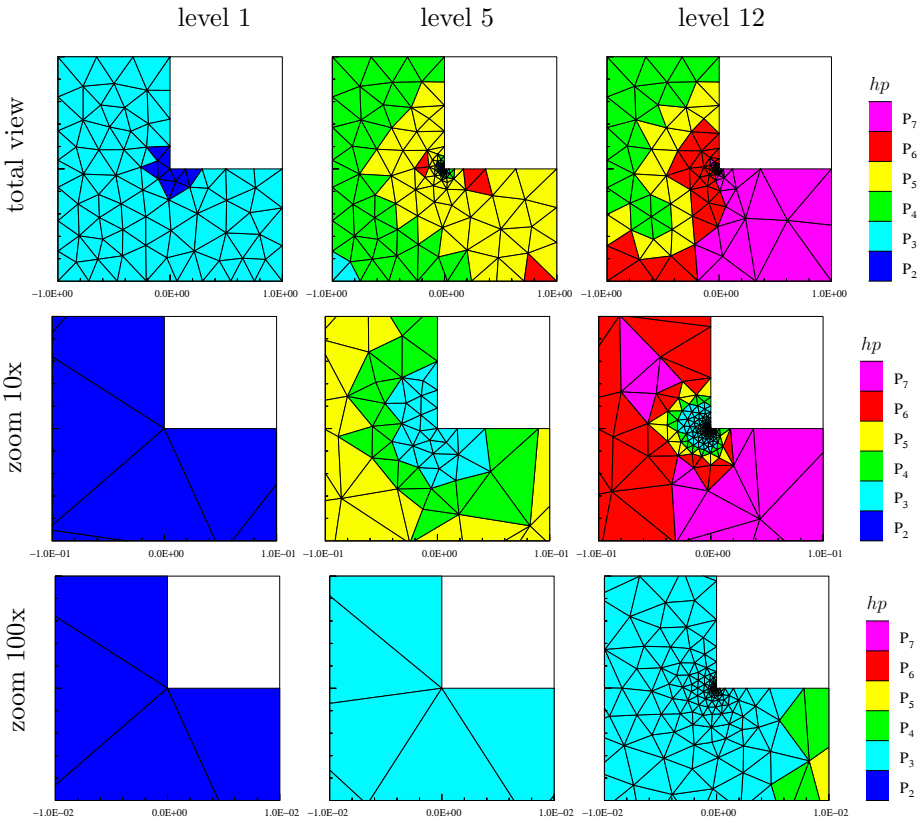

Fig. 4: Case 1, Algorithm 2: hp-grids with details around the origin; levels 1, 5, and 12

5.4 Case 3: interior line singularity

The setting is here $\Omega = (-1,1)^2$ and

$$u(x_1,x_2) = \begin{cases} \cos(\pi x_2/2) & \text{for } x_1 \le \beta(x_2-1), \\ \cos(\pi x_2/2) + (x_1 - \beta(x_2-1))^\alpha & \text{for } x_1 > \beta(x_2-1), \end{cases} \tag{5.3}$$

with $\alpha = 2$ and $\beta = 0.6$. The solution satisfies $u \in H^{\alpha+1/2-\epsilon}(\Omega)$ for all $\epsilon > 0$ and features a mild singularity along the line $x_1 - \beta(x_2-1) = 0$.

We carried out computations with $\varpi = 10^{-4}$ by both algorithms. The line singularity is difficult to capture since it is relatively weak. However, without a sufficient refinement along this line, it is not possible to decrease the computational error under the given tolerance. Figure 7 again compares η and $\|\nabla(u-u_h)\|$. The exponential order of convergence can be observed only for Algorithm 2.

Table 6 and Figure 8 finally report the error and the estimator with its components in this last case. The effectivity index takes fairly constant values comprised between 2.3 and 4.4 and we observe an h-refinement along the line singularity, which spreads only over a few elements in the direction perpendicular to this line.

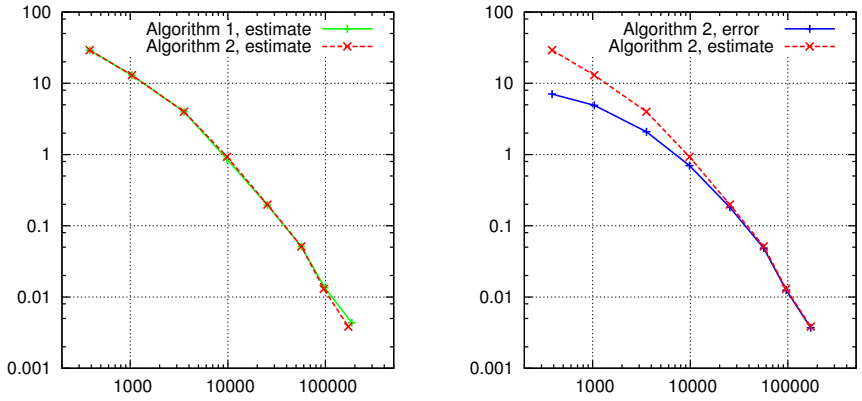

Fig. 5: Case 2, estimates η (and error $\|\nabla(u-u_h)\|$) with respect to DoF, comparison of Algorithms 1 and 2 (left) and Algorithm 2 (right)

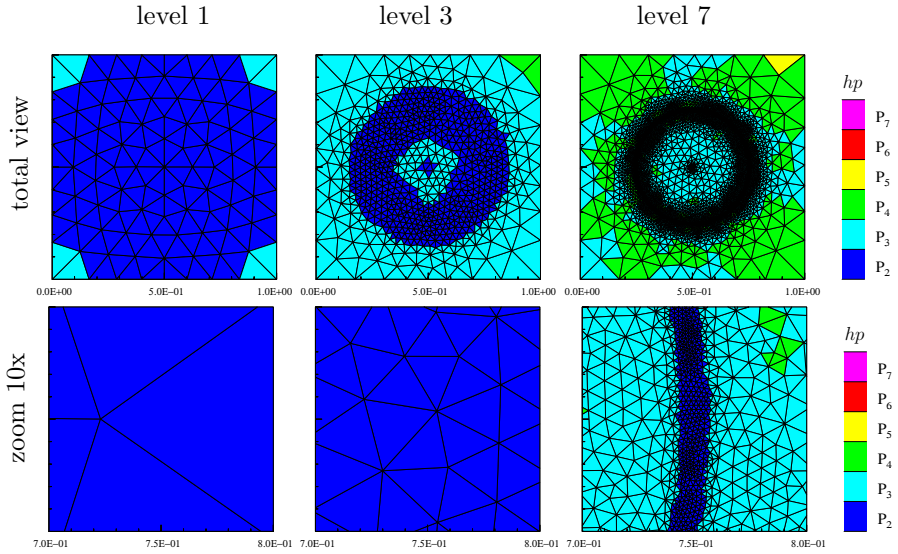

Fig. 6: Case 2, Algorithm 2: hp-grids with details along the circular front; levels 1, 3, and 7

References

[1] I. Babuška and M. Suri, *The p and h-p versions of the finite element method, basic principles and properties*, SIAM Rev., 36 (1994), pp. 578–632.

[2] D. Braess, V. Pillwein, and J. Schöberl, *Equilibrated residual error estimates are p-robust*, Comput. Methods Appl. Mech. Engrg., 198 (2009), pp. 1189–1197.

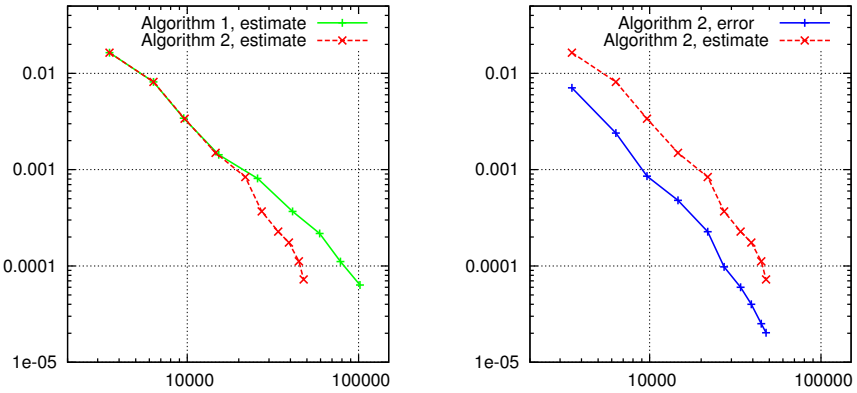

Fig. 7: Case 3, estimates η (and error $\|\nabla(u-u_h)\|$) with respect to DoF, comparison of Algorithms 1 and 2 (left) and Algorithm 2 (right)

lev	$\#\mathcal{T}_h$	DoF	$\|\nabla(u-u_h)\|$	η_{CR}	η_{osc}	η_{NC}	η_{BC}	η	I^{eff}
0	586	3516	7.07E-03	6.25E-03	1.05E-02	1.06E-03	3.70E-04	1.64E-02	2.32
1	647	6350	2.40E-03	2.02E-03	6.24E-03	1.19E-04	5.21E-05	8.16E-03	3.40
2	883	9653	8.56E-04	7.22E-04	2.69E-03	8.96E-05	1.74E-05	3.38E-03	3.95
3	1296	14646	4.80E-04	3.44E-04	1.17E-03	2.07E-05	2.71E-05	1.49E-03	3.11
4	1840	21822	2.27E-04	1.95E-04	6.49E-04	1.21E-05	2.03E-05	8.39E-04	3.70
5	2217	27218	9.78E-05	7.59E-05	2.97E-04	1.03E-05	9.17E-06	3.69E-04	3.77
6	2683	33940	6.00E-05	4.72E-05	1.82E-04	3.30E-06	2.30E-06	2.27E-04	3.79
7	3113	39196	4.00E-05	3.32E-05	1.44E-04	3.14E-06	3.15E-06	1.75E-04	4.38
8	3519	44853	2.52E-05	1.88E-05	9.57E-05	3.03E-06	3.87E-06	1.12E-04	4.44
9	3618	47837	2.02E-05	1.47E-05	5.90E-05	8.32E-07	6.85E-07	7.24E-05	3.58

Tab. 6: Case 3, Algorithm 2: convergence of the error and of the estimate and with its components

[3] D. Braess and J. Schöberl, *Equilibrated residual error estimator for edge elements*, Math. Comp., 77 (2008), pp. 651–672.

[4] S. C. Brenner, *Poincaré-Friedrichs inequalities for piecewise H^1 functions*, SIAM J. Numer. Anal., 41 (2003), pp. 306–324.

[5] F. Brezzi and M. Fortin, *Mixed and hybrid finite element methods*, vol. 15 of Springer Series in Computational Mathematics, Springer-Verlag, New York, 1991.

[6] C. Carstensen and C. Merdon, *Computational survey on a posteriori error estimators for nonconforming finite element methods for the Poisson problem*, J. Comput. Appl. Math., 249 (2013), pp. 74–94.

[7] P. G. Ciarlet, *The Finite Element Method for Elliptic Problems*, vol. 4 of Studies in Mathematics and its Applications, North-Holland, Amsterdam, 1978.

[8] M. Costabel and A. McIntosh, *On Bogovskiĭ and regularized Poincaré integral operators for de Rham complexes on Lipschitz domains*, Math. Z., 265 (2010), pp. 297–320.

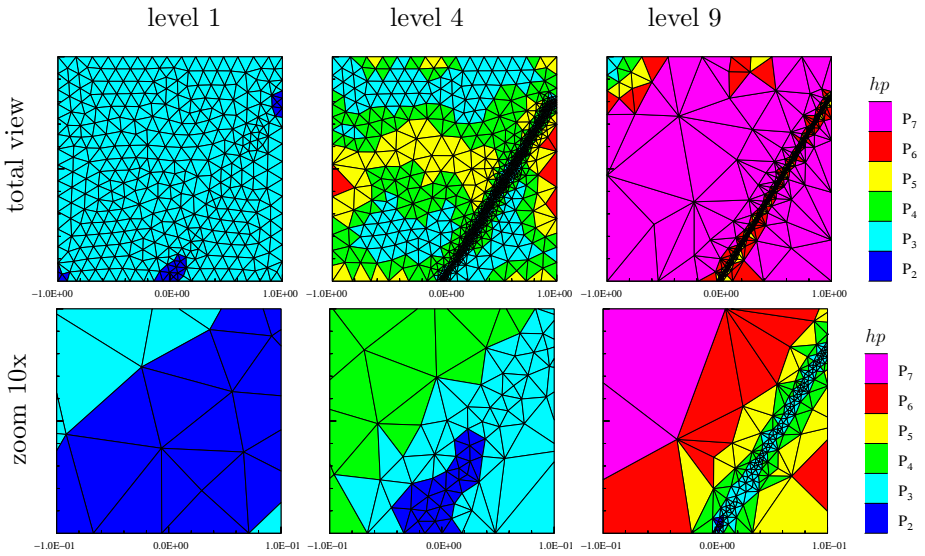

Fig. 8: Case 3, Algorithm 2: *hp*-grids with details along the interior layer; levels 1, 4, and 9

[9] L. Demkowicz, J. Gopalakrishnan, and J. Schöberl, *Polynomial extension operators. Part III*, Math. Comp., 81 (2012), pp. 1289–1326.

[10] L. Demkowicz, W. Rachowicz, and P. Devloo, *A fully automatic hp-adaptivity*, J. Sci. Comput., 17 (2002), pp. 117–142.

[11] P. Destuynder and B. Métivet, *Explicit error bounds in a conforming finite element method*, Math. Comp., 68 (1999), pp. 1379–1396.

[12] D. A. Di Pietro and A. Ern, *Mathematical Aspects of Discontinuous Galerkin Methods*, vol. 69 of Mathématiques & Applications, Springer-Verlag, Berlin, 2011.

[13] V. Dolejší, *Anisotropic mesh adaptation for finite volume and finite element methods on triangular meshes*, Comput. Vis. Sci., 1 (1998), pp. 165–178.

[14] ———, *ANGENER – software package*, Charles University Prague, Faculty of Mathematics and Physics, 2000. http://www.karlin.mff.cuni.cz/~dolejsi/angen/angen.htm.

[15] ———, *Anisotropic mesh adaptation technique for viscous flow simulation*, East-West J. Numer. Math., 9 (2001), pp. 1–24.

[16] T. Eibner and J. M. Melenk, *An adaptive strategy for hp-FEM based on testing for analyticity*, Comput. Mech., 39 (2007), pp. 575–595.

[17] A. Ern and M. Vohralík, *Adaptive inexact Newton methods with a posteriori stopping criteria for nonlinear diffusion PDEs*, SIAM J. Sci. Comput., 35 (2013), pp. A1761–A1791.

[18] ———, *Polynomial-degree-robust a posteriori estimates in a unified setting for conforming, nonconforming, discontinuous Galerkin, and mixed discretizations*, SIAM J. Numer. Anal., 53 (2015), pp. 1058–1081.

[19] W. Gui and I. Babuška, *The h, p and h-p versions of the finite element method in* 1 *dimension. III. The adaptive h-p version*, Numer. Math., 49 (1986), pp. 659–683.

[20] P. Houston and E. Süli, *A note on the design of hp–adaptive finite element methods for elliptic partial differential equations*, Comput. Methods Appl. Mech. Engrg., 194 (2005), pp. 229–243.

[21] K.-Y. Kim, *A posteriori error analysis for locally conservative mixed methods*, Math. Comp., 76 (2007), pp. 43–66.

[22] P. Ladevèze and D. Leguillon, *Error estimate procedure in the finite element method and applications*, SIAM J. Numer. Anal., 20 (1983), pp. 485–509.

[23] W. F. Mitchell, *A collection of 2D elliptic problems for testing adaptive grid refinement algorithms*, Appl. Math. Comput., 220 (2013), pp. 350–364.

[24] W. F. Mitchell and M. A. McClain, *A comparison of hp-adaptive strategies for elliptic partial differential equations*, ACM Trans. Math. Software, 41 (2014), pp. Art. 2, 39.

[25] S. Nicaise, *A posteriori error estimations of some cell-centered finite volume methods*, SIAM J. Numer. Anal., 43 (2005), pp. 1481–1503.

[26] J. E. Roberts and J.-M. Thomas, *Mixed and hybrid methods*, in Handbook of Numerical Analysis, Vol. II, North-Holland, Amsterdam, 1991, pp. 523–639.

[27] C. Schwab, *p- and hp-Finite Element Methods*, Clarendon Press, Oxford, 1998.

[28] P. Šolín, *Partial differential equations and the finite element method*, Pure and Applied Mathematics, Wiley-Interscience, New York, 2004.

[29] P. Šolín and L. Demkowicz, *Goal-oriented hp-adaptivity for elliptic problems*, Comput. Methods Appl. Mech. Engrg., 193 (2004), pp. 449–468.

[30] A. Veeser and R. Verfürth, *Poincaré constants for finite element stars*, IMA J. Numer. Anal., 32 (2012), pp. 30–47.

[31] R. Verfürth, *A posteriori error estimation techniques for finite element methods*, Numerical Mathematics and Scientific Computation, Oxford University Press, Oxford, 2013.